

Response to anonymous Referee #1

General Comments:

This paper examines recent trends in baseline carbon monoxide (CO) and ozone (O₃) in the northeast US region using measurements at seven rural sites in New England and upstate New York. The paper documents significant decreasing trends in CO while showing that there was no significant long-term trend in O₃. The authors examine in great detail the causes for these results including the impacts of changes in local and global anthropogenic emissions, wildfires and the impacts of meteorological factors such as long-range transport, clouds, temperature, humidity and stratospheric intrusions, and the relationship of these factors to climate indices including the North Atlantic Oscillation (NAS) and Arctic Oscillation (AO). Their scientific arguments are sound and because they can be used to hypothesize about the combined impacts on air quality of future changes to anthropogenic emissions and atmospheric circulation changes resulting from climate change they are highly relevant to current environmental concerns.

There are a couple scientific issues detailed in the Specific Comments section and a number of corrections listed in the Technical Corrections section that should be addressed. However, these do not detract from the overall message of the paper. Therefore I recommend that the paper be published in Atmospheric Chemistry and Physics after these minor revisions are completed.

We would like to thank the reviewer for their constructive remarks and comments on the article. Below we have responded to each one of the reviewer's comments (shaded). We have taken most of the reviewer's suggestions to improve the manuscript.

Specific Comments:

Why was the daily maximum solar radiation flux at Thompson Farm so low in spring 2002 (Figures 3 and 9b)? The NAO was positive but it was also positive in other years (e.g. 2004) without the solar radiation flux being so low.

We averaged daily maximum solar radiation flux at Thompson Farm in spring (March, April, and May), and the interannual variation was shown in Figure 3a. The difference between Figure 3a and Figure 9b was that the May data were excluded in Figure 9b. The hourly data of solar radiation flux were obtained from the Climate Reference Network (CRN) run by the National Ocean and Atmospheric Administration's (NOAA) National Centers for Environmental Information. (<http://www.ncdc.noaa.gov/crn/>). Missing data were only found on five days in spring 2002 and no mistakes were found in our calculation. It seems that there is no reason to throw out the spring 2002 data.

We compared the difference of geopotential height at 850 hPa in spring 2002 and spring 2004, and found that geopotential height over the eastern US coast was ~30 gpm higher in spring 2002 than in spring 2004 (Figure S1a). In addition, precipitable water over our study region was ~1.5 kg m⁻² more in spring 2002 than in spring 2004. The NAO index was positive in spring 2002 and spring 2004 (Figure 9a). The geopotential height over the Bermuda high and

the eastern US coast was significantly higher in positive NAO years than in negative NAO years (Figure 10). Rogers (1997) suggested that the North Atlantic storm track paralleled the eastern North American coastline during positive NAO years. With higher geopotential height at 850 hPa over the eastern US coast in spring 2002 (Figure S1a), storm tracks could possibly be more parallel to the east coast in 2002 than in 2004. Consequently, stronger transport of moisture and wet conditions near the eastern US coast (Figure S1b) could lead to more cloudiness and lower solar radiation flux in spring 2002. Further research is needed to fully understand what may have caused the very low solar radiation flux in spring 2002.

We added “More frequent cyclone activities, wetter conditions associated with the North Atlantic storm track parallel to the eastern US coast could be possible factors leading to the very low solar radiation flux in spring 2002. Further research is warranted to fully understand what may have caused this phenomenon.” in L509 – L512.

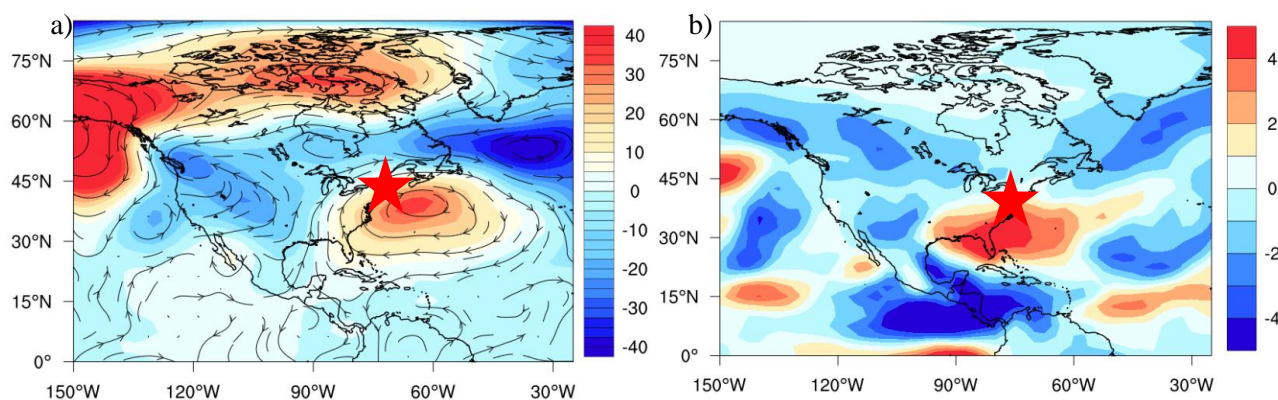


Figure S1. (a) The difference of geopotential height at 850 hPa and (b) precipitable water (kg m^{-2}) between spring 2002 and spring 2004.

In Section 3.3.3 the authors show that the NAO does not play a significant role in the interannual variability of baseline CO. Later in the section the authors suggest, citing other studies, that the circulation pattern associated with the positive NAO may work to lower baseline O₃ in the northeast US by facilitating continental export. However, wouldn't those same mechanisms also facilitate export of CO limiting its buildup? Do these findings suggest that the impact of continental export on O₃ is small compared to the impacts of decreased stratospheric intrusions and solar radiation flux?

Thank you for this interesting comment. It inspired us to think more deeply about the impact of NAO on air quality in the Northeast US.

Averaged westerly wind speed (247.5–337.5°) was positively correlated with the NAO index at most of our study sites (MWO: $r = 0.76$, $p = 0.02$; CS: $r = 0.68$, $p = 0.06$; TF: $r = 0.57$, $p = 0.09$) (Table 4 and Figure 9c), suggesting that North American continental export could be one factor contributing to the negative correlation between baseline O₃ and the NAO index. Negative correlation, although insignificant, was also found between baseline CO and the NAO index (Table 4). Some studies (Creilson et al., 2003; Eckhardt et al., 2004; Stohl et al., 2003) also suggested that transport of particular matter, O₃ and its precursors from North

America to Europe was enhanced during positive NAO years. In addition, positive NAO years were accompanied by less stratospheric intrusion, potentially weakening a source of surface O₃ and subsequently decreasing baseline O₃ levels. However, less stratospheric intrusion could also lead to less dilution of surface CO and thus increase baseline CO levels. The opposite effects of factors such as stratospheric intrusion and continental export could complicate the relationship between the NAO and baseline CO. Without model simulations, it is hard to delineate such effects as well as to quantify the relative contributions of the three factors (export of ozone, stratospheric intrusion, and solar radiation flux) to the variation of baseline O₃.

The text was revised to reflect these thoughts. The statement “it should be noted that, no significant correlation was found between the NAO index and baseline CO at any of the sites, which suggests that NAO is not linked to or played an insignificant role in the interannual variability of baseline CO.” was deleted (L693). Instead, we added “Negative correlation, although insignificant, was also found between baseline CO and the NAO index at most of our study sites (Table 4). North American continental export could also impact the variation of baseline CO, while this impact could be confounded by other factors, e.g. stratospheric intrusion. Specifically, during positive NAO years, more continental outflows lead to a decrease in baseline CO, while less stratospheric intrusion would lead to less dilution of surface CO and thus increase baseline CO levels. Further research is warranted to fully understand the relationship between baseline CO and NAO.” (L743 – L749)

Technical Corrections:

Thanks for spotting these errors. They have been corrected.

Page 27254, Line 1:

You should define baseline CO and O₃ at the beginning of the abstract to inform the reader that it is not exactly the same as the background. The first sentence of the abstract could be something like “We define a baseline CO as the lowest 20th percentile of mixing ratios and a baseline O₃ as that corresponding to the baseline CO.”

Baseline CO and O₃ were originally defined in the Introduction (L105). To inform the reader earlier and more clearly, the definition of baseline CO and O₃ was also added to the beginning of the abstract.

“Baseline carbon monoxide (CO) and ozone (O₃) were defined as mixing ratios of CO and O₃ under minimal influence of recent and local emissions. In this study, baseline carbon monoxide (CO) and ozone (O₃) were examined at seven rural sites in the Northeast US during varying periods over 2001–2010. Specifically, baseline air was determined using the monthly 10th percentile level of CO at Appledore Island (AI), Castle Spring (CS), Pack Monadnock (PM), Thompson Farm (TF), Pinnacle State Park (PSP), and 50th percentile level at Mt. Washington (MWO) and Whiteface Mountain (WFM). Monthly median O₃ levels of the baseline air were defined as baseline O₃ levels.” (L28 – L35)

Page 27255, Line 2: Add a period after US.

Added “over 2001–2010”. (L60)

Page 27255 starting at Line 13: Consider swapping the order of the first two paragraphs in the introduction to be consistent with the title and the abstract (i.e. CO is discussed before O₃).

Revised as suggested. (L74 – L88)

Page 27256, Lines 25 -26: Change “could be transported downwind and subsequently affect the baseline CO and O₃ levels there” to “could affect the baseline CO and O₃ levels downwind.”

Revised as suggested. (L130)

Page 27257, Line 3: Consider mentioning the new stricter EPA standards governing O₃ exceedances.

We discussed the new EPA O₃ standards in the Summary (L771 – L775). To avoid repeating the discussion, we would like to briefly mention the NAAQS here. (L136)

Page 27257, Line 5: Change “mid-latitudes” to “mid-latitude regions”.

Changed. (L139)

Page 27257, Lines 5 – 8: Consider combining the two sentences into one with the clause “and no consistent trends” after “Asia” to connect the two thoughts. The reference list should then be moved to the end of the new sentence.

Revised as suggested (L138 – L142).

“Studies have been conducted to investigate trends in baseline CO and O₃ across northern hemispheric mid-latitudes regions, such as North America, Europe, and Asia, and no consistent trends have been found (Chan, 2009; Cooper et al., 2010; Cui et al., 2011; Logan et al., 2012; Oltmans et al., 2013; Parrish et al., 2012; Tilmes et al., 2012; Wilson et al., 2012; Xu et al., 2008).”

Page 27257, Lines 28 -29: This is a bit confusing since you start the sentence with “Most studies” but only list two and “episode” is singular.

We would like to point that most studies investigated the impact of wildfires during a few days. Our work was to examine the long-term impact of wildfires.

We changed “Most studies demonstrated elevated CO and O₃ due to fire emissions for an episode (e.g., Dutkiewicz et al., 2011; Honrath et al., 2004).” to “Most studies focused on episodic enhancements in CO and O₃ linked to fire emissions (e.g., DeBell et al., 2004; Dutkiewicz et al., 2011; Honrath et al., 2004).” (L160 – L163)

Page 27258, Line 2: Change after “O₃” to “, and both of these focused on ten years of observations from the 1990s.”

Revised to “To the best of our knowledge, only two studies (Jaffe et al., 2004; Wotawa et al., 2001) examined the impact of wildfires on baseline CO and O₃ over time periods of ten years in the 1990s. Thus, more research is warranted to investigate the impact of wildfires on baseline CO and O₃ on decadal scales” (L163 – L165)

Page 27258, Line 3: Change “More” to “Thus more”.

Added “Thus”. (L165)

Page 27258, Line 16: Add a period after “US”.

Added “over 2001 – 2010”. (L178)

Page 27258, Line 28: Insert “with” before “less”.

Added. (L189)

Page 27259, Line 9: Hegarty et al., 2007 is the correct reference.

Changed. (L197)

Page 27261, Line 21: Add “and” before “potential”.

Added “and”. (L258)

Page 27262, Line 13: The meaning of the clause “the center of a cyclone was obtained” seems unclear in this context. Do you mean that if more than one local minimum is found the cyclone position is designated as the center point of the local minima?

There might be several local minima within 720 km. In our algorithm, only the lowest sea level pressure was obtained as the continuation of the previous cyclone.

“the center of a cyclone was obtained” was replaced by “the point with the lowest sea level pressure was designated as the center of a cyclone”. (L278)

Page 27264 Lines 25 – 30, and Page 27296, Table 2: I think the numbers in the “Annual CO” column in Table 2 have the wrong sign (positive) except for CS which should be positive. Please check and correct where necessary. Also please check the “Annual O₃” column. Based on the seasonal trends it looks like some of the annual trend should be negative but they are all listed as positive.

All numbers in Table 2 were double-checked and errors corrected.

Page 27275, Line 7: Add a period after “US” and capitalize “of”.

Changed. (L605)

Page 27276, Line 5: Change “ultimate” to “ultimately”.

Changed. (L628)

Page 27278, Line 14: Change “known as the positive phase of NAO” to “which is indicative of the positive phase of the NAQ”.

Changed. (L686)

Page 27281, Lines 18 - 20: On October 1, 2015 the EPA lowered the 8-hour average O₃ standard to 70 ppbv (<http://www3.epa.gov/ozonepollution/pdfs/20151001overviewfs.pdf>). Please update this sentence.

Changed to “On 1 October 2015 the U.S. EPA lowered the NAAQS for ground-level O₃ to 70 ppbv to improve protection of public health and welfare (<http://www3.epa.gov/ozonepollution/pdfs/20151001overviewfs.pdf>).” (L771– L775)

References

Creilson, J. K., Fishman, J. and Wozniak, a. E.: Intercontinental transport of tropospheric ozone: A study of its seasonal variability across the North Atlantic utilizing tropospheric ozone residuals and its relationship to the North Atlantic Oscillation, *Atmospheric Chem. Phys. Discuss.*, 3(4), 4431–4460, doi:10.5194/acpd-3-4431-2003, 2003.

Eckhardt, S., Stohl, A., Wernli, H., James, P., Forster, C. and Spichtinger, N.: A 15-year climatology of warm conveyor belts, *J. Clim.*, 17(1), 218–237, 2004.

Rogers, J. C.: North Atlantic storm track variability and its association to the North Atlantic oscillation and climate variability of Northern Europe, *J. Clim.*, 10(7), 1635–1647, doi:10.1175/1520-0442(1997)010<1635:NASTVA>2.0.CO;2, 1997.

Stohl, A., Huntrieser, H., Richter, A., Beirle, S., Cooper, O. R., Eckhardt, S., Forster, C., James, P., Spichtinger, N., Wenig, M., Wagner, T., Burrows, J. P. and Platt, U.: Rapid intercontinental air pollution transport associated with a meteorological bomb, *Atmospheric Chem. Phys.*, 3(4), 969–985, 2003.

1 **Regional and Hemispheric Influences on Variability and Trends of Baseline**
2 **Carbon Monoxide and Ozone over the Northeast US**~~Baseline—carbon~~
3 **monoxide and ozone in the northeast US over 2001–2010**

4 **Y. Zhou¹, H. Mao¹, K. Demerjian², C. Hogrefe³, and J. Liu^{4,5}**

5 ¹ Department of Chemistry, State University of New York College of Environmental Science and
6 Forestry, Syracuse, NY 13210, USA

7 ² Atmospheric Science Research Center, State University of New York at Albany, Albany, NY
8 12203, USA

9 ³ Emissions and Model Evaluation Branch, Atmospheric Modeling and Analysis Division,
10 NERL, ORD, U.S. EPA, Research Triangle Park, NC 27711, USA

11 ⁴ School of Atmospheric Sciences, Nanjing University, Nanjing, 210093, China

12 ⁵ Department of Geography and ~~Program in~~ Planning, University of Toronto, ~~100 St. George~~
13 ~~Street,~~ Toronto, ON M5S 3G3, Canada

14 Received: 17 August 2015 – Accepted: 5 September 2015 – Published: 8 October 2015

15 Correspondence to: Y. Zhou (yzhou51@syr.edu)

16 Published by Copernicus Publications on behalf of the European Geosciences Union.

17

18

19

20

21

22

23

24

25

26

27 **Abstract**

28 Baseline carbon monoxide (CO) and ozone (O₃) were defined as mixing ratios of CO and O₃
29 under minimal influence of recent and local emissions. In this study, ~~Baseline~~-baseline carbon
30 monoxide (CO) and ozone (O₃) were ~~examined~~studied at seven rural sites in the northeast US
31 during varying periods over 2001–2010. ~~Specifically, baseline air was determined using the~~
32 monthly 10th percentile level of CO at Appledore Island (AI), Castle Spring (CS), Pack
33 Monadnock (PM), Thompson Farm (TF), Pinnacle State Park (PSP), and 50th percentile level at
34 Mt. Washington (MWO) and Whiteface Mountain (WFM). Monthly median O₃ levels of the
35 baseline air were defined as baseline O₃ levels. Interannual and seasonal variations of baseline
36 CO and O₃ were examined for the effects of changes in anthropogenic emissions, stratospheric
37 intrusion, transport pathways and O₃ photochemistry. Baseline CO generally exhibited
38 decreasing trends at most sites, except at ~~Castle Spring (CS)~~, an elevated (~ 400 ma.s.l.) site in
39 rural central New Hampshire. Over April 2001–December 2010, baseline CO at ~~Thompson Farm~~
40 ~~(TF)~~, ~~Pinnacle State Park (PSP)~~, and ~~Whiteface Mountain (WFM)~~ decreased at rates ranging
41 from -4.3 to -2.5 ppbv yr⁻¹. Baseline CO decreased significantly at a rate of -2.3 ppbv yr⁻¹ at
42 ~~Mt. Washington (MWO)~~ over April 2001–March 2009, and -3.5 ppbv yr⁻¹ at ~~Pack Monadnock~~
43 ~~(PM)~~ over July 2004–October 2010. Unlike baseline CO, baseline O₃ did not display a
44 significant long term trend at any of the sites, resulting probably from opposite trends in NO_x
45 emissions worldwide and possibly from the overall relatively constant mixing ratios of CH₄ in
46 the 2000s. In looking into long term trends by season, wintertime baseline CO at MWO and
47 WFM, the highest sites, did not exhibit a significant trend, probably due to the competing effects
48 of decreasing CO emissions in the US and increasing emissions in Asia. Springtime and
49 wintertime baseline O₃ at TF increased significantly at a rate of 2.4 and 2.7 ppbv yr⁻¹,

50 respectively, which was likely linked to nitrogen oxides (NO_x) emissions reductions over urban
51 areas and possible resultant increases in O_3 due to less titration by NO in urban plumes. The
52 effects of meteorology on baseline O_3 and CO were investigated. A negative correlation was
53 found between springtime baseline O_3 and the North Atlantic oscillation (NAO) index. It was
54 found that during positive NAO years, lower baseline O_3 in the northeast US was linked to less
55 solar radiation flux, weakened stratospheric intrusion, and intensified continental export. The
56 lowest baseline CO at ~~Appledore Island (AI)~~, PM, TF, PSP, WFM and the lowest baseline O_3 at
57 AI, PM, and PSP in summer 2009 were linked to the negative phase of the Arctic oscillation
58 (AO), when more frequent cyclone activities brought more clean Arctic air to midlatitudes. It
59 was also found that forest fires played a major role in determining baseline CO in the northeast
60 US over 2001–2010. In summer, ~ 38 % of baseline CO variability at AI, CS, MWO, TF, PSP,
61 and WFM could be explained by CO emissions from forest fires in Russia and ~ 22 % by
62 emissions from forest fires in Canada. Long-range transport of O_3 and its precursors from
63 biomass burning contributed to the highest baseline O_3 in summer 2003 at AI, CS, MWO, TF,
64 and WFM. The findings of this study suggested impacts of increasing Asian emissions, NO_x
65 emissions from the Northeast Urban corridor, global biomass burning emissions, and
66 meteorological conditions (e.g. cyclone activity, AO, and NAO) should all be considered when
67 designing strategies for meeting and maintaining National Ambient Air Quality Standards
68 (NAAQS) and evaluating the air quality in the northeast US.

69

70

71

72

1 Introduction

Carbon monoxide (CO) is a product of incomplete combustion (e.g. fossil fuel, biofuel, and biomass burning) and oxidation of hydrocarbon compounds (Worden et al., 2013). CO is a major sink of hydroxyl radicals (OH), and hence changes in CO can impact many chemically important trace species that are removed via oxidation by OH (Daniel and Solomon, 1998; Petrenko et al., 2013). In the presence of nitrogen oxides (NO_x), CO oxidation is important in the tropospheric ozone (O₃) budget. Due to its relatively unreactive chemical nature, CO has been used as a tracer of anthropogenic influence and fire emissions (Gratz et al., 2014; Price et al., 2004; Weiss-Penzias et al., 2006).

Tropospheric ~~ozone (O₃)~~, which is produced largely by photochemical oxidation of ~~nitrogen oxides (NO_x)~~ and volatile organic compounds (VOCs), is a serious and ubiquitous air pollutant affecting humans' respiratory system, reducing yields of agricultural crops, and damaging natural ecosystems (EPA, 2012). As a precursor of ~~hydroxyl radicals (OH)~~, a dominant oxidant, O₃ regulates the atmospheric capacity of oxidation (Prinn, 2003). Tropospheric O₃ is also the third strongest greenhouse gas, after carbon dioxide (CO₂) and methane (CH₄), suggested by the Intergovernmental Panel on Climate Change (IPCC, 2007).

~~CO is a product of incomplete combustion (e.g. fossil fuel, biofuel, and biomass burning) and oxidation of hydrocarbon compounds (Worden et al., 2013). CO is a major sink of OH, and hence changes in CO can impact many chemically important trace species that are removed via oxidation by OH (Daniel and Solomon, 1998; Petrenko et al., 2013). In the presence of NO_x, CO oxidation is important in the tropospheric O₃ budget. Due to its relatively unreactive chemical nature, CO has been used as a tracer of anthropogenic influence and fire emissions (Gratz et al., 2014; Price et al., 2004; Weiss-Penzias et al., 2006).~~

96 The United States has made enormous efforts to control ambient mixing ratios of criteria
97 pollutants since the 1970s (EPA, 2012). Nationally, annual second maximum 8 h average mixing
98 ratios of CO decreased by 52 %, and annual mean mixing ratios of nitrogen dioxide (NO₂)
99 declined by 33 % over 2001–2010 (EPA, 2012). Ambient O₃ concentrations in metropolitan
100 areas, such as Los Angeles, New York City, and Chicago, decreased significantly in the past two
101 decades (Bell et al., 2007; Cooper et al., 2010, 2012; Lefohn et al., 2010; Parrish et al., 2011).
102 Despite the decreasing anthropogenic emissions in Europe and North America, emissions in
103 China and India have increased. Biomass burning emissions vary both spatially and temporally
104 (Granier et al., 2011; Gratz et al., 2014). It remains unclear how such opposing changes in
105 emissions have globally affected baseline CO and O₃, which are defined as mixing ratios of CO
106 and O₃ under minimal influence of recent and local emissions (Chan and Vet, 2010; HTAP,
107 2010).

108 Background or baseline has been used, often interchangeably, to quantify how much O₃
109 produced from recent or local anthropogenic emissions could be allowed to attain the O₃
110 standards (HTAP, 2010; Huang et al., 2015). A few recent studies discussed the difference
111 between background O₃ and baseline O₃ (HTAP, 2010; Huang et al., 2015; Parrish et al., 2012;
112 Chan et al., 2010). The term “background” was used in modeling studies that estimated the
113 atmospheric mixing ratio of a compound determined by natural sources only, while the term
114 “baseline” was obtained from measurement records by removing data of local influences (HTAP,
115 2010, Chan et al., 2010; Parrish et al., 2012). Quantitative estimates of baseline CO and O₃ are
116 not straightforward since measurements at a particular location include contributions from local
117 anthropogenic precursor emissions (Chan and Vet, 2010). Various methods have been utilized to
118 diagnose baseline conditions, including using measurements at remote sites, analysis of the

119 probability distribution of pollutants, correlations with reactive nitrogen oxides, and isentropic
120 back-trajectories (e.g., Altshuller and Lefohn, 1996; Lin et al., 2000; Jaffe et al., 2003; Derwent
121 et al., 2007; Parrish et al., 2009; Cui et al., 2011; Wilson et al., 2012). ~~In the literature, Air~~
122 masses with low percentile values (< 20th percentile in the literature) of CO, an excellent
123 anthropogenic tracer for its origin of mobile combustion, are commonly considered background
124 baseline air (e.g., Lin et al., 2000; Mao and Talbot, 2012). Based on Lin et al. (2000), ~~t~~The low
125 percentile value of CO is used as baseline CO, and baseline O₃ is then estimated using the data
126 corresponding to CO mixing ratios below the baseline CO level ~~(e.g., Lin et al., 2000; Mao and~~
127 ~~Talbot, 2012).~~

128 The lifetime of CO and O₃ in the free troposphere is ~ 2 months and ~ 20 days,
129 respectively (Price et al., 2004; Stevenson et al., 2006). Thus, CO, O₃, and other precursors
130 emitted in the upwind region and those produced in transit could affect the baseline CO and O₃
131 levels there~~be transported downwind and subsequently affect the baseline CO and O₃ levels there~~
132 (Cooper et al., 2012; Oltmans et al., 2008; Pollack et al., 2013). This has important regulatory
133 implications, because the levels of baseline CO and O₃ directly affect emission control of CO
134 and other O₃ precursors. Therefore, quantifying trends and variations in baseline CO and O₃ is of
135 vital importance to assessing air quality and designing cost-effective emission control plans to
136 meet the National Ambient Air Quality Standards (NAAQS)
137 (<http://www3.epa.gov/ttn/naaqs/criteria.html>).

138 Studies have been conducted to investigate trends in baseline CO and O₃ across northern
139 hemispheric mid-latitudes regions, such as North America, Europe, and Asia, and no consistent
140 trends have been found (Chan, 2009; Cooper et al., 2010; Cui et al., 2011; Logan et al., 2012;
141 Oltmans et al., 2013; Parrish et al., 2012; Tilmes et al., 2012; Wilson et al., 2012; Xu et al.,

142 | 2008). ~~No consistent trends have been found.~~ Kumar et al. (2013) reported trends of -0.31 and
143 -0.21 ppbv yr^{-1} for CO and O₃, respectively, at the Pico Mountain Observatory over 2001–2011.
144 Gratz et al. (2014) reported that the springtime median mixing ratio of O₃ increased at a rate of
145 0.76 ppbv yr^{-1} at the Mt. Bachelor Observatory over 2004–2013, while median CO decreased at
146 a rate of -3.1 ppbv yr^{-1} . Chan and Vet (2010) found that baseline O₃ in the eastern US decreased
147 in spring, summer, and fall over 1997–2006, and the decadal trends in the Atlantic coastal region
148 were positive in winter, summer, and fall. For the most part, causes for temporal variability have
149 not been adequately explained. Interpretation of long-term trends is difficult because of
150 significant interannual variability in emissions and climate as well as possibly in photochemistry
151 (Hess and Lamarque, 2007). Climate change may lead to changes in natural emissions (e.g.,
152 emissions from wildfires, vegetation, and lightning), pollution transport pathways, and
153 stratosphere-tropospheric exchange (Parrish et al., 2013).

154 Wildfires release large quantities of O₃ precursors, e.g., CO, VOCs, and NO_x, every year.
155 For instance, the MACCity emission inventory over 2001–2010 suggested that total global
156 biomass burning emissions of CO ranged from ~ 300 to ~ 460 Tg yr^{-1} , close to ~ 590 Tg yr^{-1}
157 anthropogenic emissions (Granier et al., 2011). These chemical species could make a significant
158 contribution to tropospheric CO and O₃ budgets, impacting the interannual variability of surface
159 CO and O₃ globally (Dutkiewicz et al., 2011; Herron-Thorpe et al., 2014; Honrath et al., 2004;
160 Kang et al., 2014; Wigder et al., 2013; Wotawa and Trainer, 2000). Most studies focused on
161 episodic enhancements in demonstrated elevated CO and O₃ linked to due to fire emissions
162 studies (e.g., DeBell et al., 2004; Dutkiewicz et al., 2011; Honrath et al., 2004) for an episode
163 (Dutkiewicz et al., 2011; Honrath et al., 2004). To the best of our knowledge, only two studies
164 (Jaffe et al., 2004; Wotawa et al., 2001) examined/quantified the impact of wildfires on baseline

165 | CO and O₃ over time periods of ten years in the 1990s ~~using ten-year observations~~. Thus mMore
166 | research is warranted to determine the impact of wildfires on baseline CO and O₃ in the 2000s in
167 | northern hemispheric midlatitudes.

168 | Regional climatic processes over the US east coast are influenced by the North Atlantic
169 | Oscillation (NAO) and the Arctic Oscillation (AO) (Archambault et al., 2008; Hess and
170 | Lamarque, 2007). Studies suggested a link between NAO and regional distributions of
171 | tropospheric trace gases over the northwestern Atlantic Ocean, northern Europe, and the Arctic
172 | region based on model simulations or measurements (Christoudias et al., 2012; Creilson et al.,
173 | 2003; Duncan and Bey, 2004; Eckhardt et al., 2003; Hegarty et al., 2009; Krichak and Alpert,
174 | 2005; Li et al., 2002; Pausata et al., 2012; Woollings and Blackburn, 2012). Most studies
175 | suggested that trace gases over North America could be transported across the Atlantic Ocean to
176 | northern Europe during the high NAO phase, particularly in winter and spring. However, to the
177 | best of our knowledge, nearly no studies examined the relationship between NAO and trace
178 | | gases over the northeast US over 2001 – 2010. Circulation patterns can not only impact the
179 | transport of pollutants to the targeted region but can also influence the export from the upwind
180 | region. Hence, upwind trace gases are also likely to change in response to varying intensity of
181 | NAO.

182 | The AO is another dominant mode of meteorological variability in the Northern
183 | Hemisphere (Creilson et al., 2005; Hess and Lamarque, 2007; Pausata et al., 2012). AO is
184 | characterized by winds circulating counterclockwise around the Arctic at around 55°N latitude,
185 | (Thompson and Wallace, 2000). In a positive AO phase, surface pressure in the polar region is
186 | abnormally low and strong winds around the pole confine cold air masses in the Arctic region;
187 | | otherwise, more Arctic cold air dives south and increases storminess in the mid-latitudes regions

188 (Thompson and Wallace, 2000). Oswald et al. (2015) hypothesized that observed higher
189 summertime O₃ levels in the northeast US was associated with less storminess in a positive AO
190 phase. Some modeling studies suggested a weak impact from stratosphere-tropospheric exchange
191 of O₃ on the lower troposphere over the Atlantic basin during a positive AO year (Brand et al.,
192 2008; Hess and Lamarque, 2007; Lamarque and Hess, 2004). The impact of AO on surface O₃ in
193 the northeast US needs to be further investigated using long-term surface measurement data.

194 Our study used long-term observations at seven rural sites in the Northeast US. Five are
195 located in rural New Hampshire (NH) and two are in rural New York (NY) State. Although
196 numerous studies have been conducted to understand the distributions of surface CO and O₃ in
197 the northeast US and their controlling mechanisms (e.g. Bae et al., 2011; Hegarty et al., 2007⁹;
198 Lai et al., 2012; Mao and Talbot, 2004; Schwab et al., 2009; Zhou et al., 2007), little work was
199 done on baseline CO and O₃ using long-term measurement data for the region. Here, the trends
200 of baseline CO and O₃ were examined at each site for the time period of 2001–2010, and
201 regional to global emissions and large scale circulation patterns were investigated for their roles
202 in the interannual and seasonal variation of baseline CO and O₃.

203 **2 Methods and data**

204 **2.1 Measurement data**

205 The seven rural sites selected in this study (Table 1 and Fig. 1) are within a few hundred
206 kilometers of each other. Their elevation varies between 18 and 2100 m. Measurements of CO,
207 O₃, wind direction, wind speed, and relative humidity at Appledore Island (AI), Castle Spring
208 (CS), Mount Washington (MWO), Pack Monadnock (PM), and Thompson Farm (TF) were
209 conducted by the University of New Hampshire (UNH) AIRMAP Observing Network
210 (<http://www.eos.unh.edu/observatories/data.shtml>). The time resolution of the continuous year-

211 round measurements at these five sites was one minute. At AI, CO was measured seasonally
212 from May to September over 2001–2006 and year round over 2007–2011, and O₃ was measured
213 seasonally from May to September over 2002–2007 and year-round over 2008–2011. All of the
214 measurements have undergone rigorous quality controls and tThe description of CO and O₃
215 measurement techniques from the UNH AIRMAP sites can be found in Mao and Talbot (2004).
216 Additionally, hourly data of solar radiation flux were available at TF over January 2002–
217 December 2010 from the Climate Reference Network (CRN) run by the National Ocean and
218 Atmospheric Administration (NOAA) (<http://www.ncdc.noaa.gov/crn/data-access>). The one-
219 hour measurement data of CO, O₃, wind direction, wind speed, and relative humidity at
220 Whiteface Mountain (WFM) and Pinnacle State Park (PSP) began around 1996 (Table 1). The
221 description of CO and O₃ measurement techniques for WFM and PSP can be found in Brandt et
222 al. (2015) and Schwab et al. (2009). The time in all of the datasets was expressed in coordinated
223 universal time (UTC), i.e. local time +5 h for non-daylight saving time and +4 h for daylight
224 saving time (March–November).

225 **2.2 Quantification of baseline CO and O₃**

226 The local afternoon time window (18:00–24:00 UTC) was selected to avoid including the
227 data representing nighttime depletion of O₃ due to dry deposition and titration (Talbot et al.,
228 2005). The planetary boundary layer (PBL) is well mixed in the afternoon. The monthly 10th
229 percentile mixing ratio of CO at AI, CS, PM, TF, and PSP was used to represent the baseline CO
230 levels. As MWO and WFM are located atop the mountains, they are far less impacted by local
231 anthropogenic emissions. Therefore, monthly median values of CO were selected at MWO and
232 WFM to represent the baseline level. To determine baseline O₃ levels, we first created a subset of
233 O₃ data by using the O₃ mixing ratios corresponding to CO mixing ratios below the monthly 10th

234 percentile values at AI, CS, PM, TF, and PSP and monthly median values at MWO and WFM.
235 The monthly median values of this subset were then defined as the baseline O₃ levels for
236 respective sites.

237 **2.3 Datasets**

238 The NAO index is a measure of the intensity of NAO, which is defined based on the leading
239 empirical orthogonal function of the normalized sea level pressure difference between the
240 subtropical high and the subpolar low using the National Centers for Environmental
241 Prediction/National Center for Atmospheric Research (NCEP/NCAR) reanalysis (Barnston and
242 Livezey, 1987). The AO index was obtained by projecting the daily 1000 hPa geopotential height
243 anomalies poleward of 20°N onto the loading pattern of the AO (Thompson and Wallace, 2000).
244 The Climate Prediction Center of NCEP ([http://www.cpc.ncep.noaa.gov/data/teledoc/
245 telecontents.shtml](http://www.cpc.ncep.noaa.gov/data/teledoc/telecontents.shtml)) routinely monitors the primary teleconnection patterns. Monthly climate
246 index values of NAO and AO were used in this study to understand the roles of global transport
247 of atmospheric species via large-scale atmospheric circulation.

248 The Global Fire Emission Data (GFED) combines satellite information of fire activities
249 and vegetation productivities, and contains the gridded monthly burned area and fire emissions.
250 GFED 3 (<http://www.globalfiredata.org/>) was used in this study to estimate the biomass burning
251 emissions of CO over Russia, Canada, California, and Alaska. Data were available for 2001–
252 2010 at 0.5° × 0.5° horizontal resolution. Monthly mean global CO columns with 1° × 1° resolution
253 obtained from the Measurements of Pollution in the Troposphere (MOPITT) instrument on the
254 satellite Terra (<https://www2.acd.ucar.edu/mopitt/>) were used for the time period of 2001–2010
255 over grids containing Russia, Canada, Alaska, and California, when wildfire CO emissions in
256 these grids calculated from GFED were larger than 1 g m⁻² month⁻¹.

257 Monthly wind, geopotential height, temperature, relative humidity ([http://www.esrl.noaa.](http://www.esrl.noaa.gov/psd/data/gridded/data.ncep.reanalysis.html)
258 [gov/psd/data/gridded/data.ncep.reanalysis.html](http://www.esrl.noaa.gov/psd/data/gridded/data.ncep.reanalysis.html)), and potential vorticity (PV) ([http://rda.ucar.edu/](http://rda.ucar.edu/datasets/ds090.0)
259 [datasets/ds090.0](http://rda.ucar.edu/datasets/ds090.0)) with a spatial resolution of $2.5^{\circ} \times 2.5^{\circ}$ from the NCEP/NCAR Global Reanalysis
260 Products were used for meteorological conditions and for identifying stratospheric intrusion.

261 The dataset representing O_3 of stratospheric origin, constructed by Liu et al. (2013)
262 (<ftp://es-ee.tor.ec.gc.ca/pub/ftpdt/Stratospheric%20Climatology/>), was also used to verify the
263 contribution of stratospheric O_3 to the two mountain sites and the decadal trends there. This
264 dataset included monthly amounts of stratospheric O_3 from the surface to 26 km altitude with $5^{\circ} \times$
265 $5^{\circ} \times 1$ km spatial resolution from the 1960s to the 2000s.

266 Mean sea level pressure data were obtained from NCEP-DOE Reanalysis 2
267 (<http://www.esrl.noaa.gov/psd/data/gridded/data.ncep.reanalysis2.html>). The dataset is six hourly
268 with a spatial resolution of $2.5^{\circ} \times 2.5^{\circ}$. The data were used to identify and quantify the cyclones
269 that passed over the northeast US.

270 **2.4 Mid-latitude cyclone identification and tracking**

271 Many algorithms have been developed since the 1970s to identify mid-latitude cyclones
272 (Hu et al., 2004; Murazaki and Hess, 2006; Racherla and Adams, 2008). The algorithm
273 developed by Bauer and Del Genio (2006) was adopted in this study to track the sea level
274 pressure minima. The first step of the algorithm was to search for the local minimum by a 2 grids
275 $\times 2$ grids matrix. The next step was to search for the local (within 720 km) minimum in the next
276 6 h time step, assuming that a cyclone cannot move faster than 120 km h^{-1} , the same criterion
277 used by Bauer and Del Genio (2006). If more than one local minimum was found, the point with
278 the lowest sea level pressure was designated as the center of a cyclone.~~the center of a cyclone~~
279 ~~was obtained.~~ Two more criteria were applied, its duration > 24 h and central pressure ≤ 1020

280 hPa. Long-term cyclone frequency statistics were calculated for the northeast US (37.5–47.5°N,
281 67.5–82.5°W).

282 **2.5 Statistical methods**

283 The open-air package in the statistical programming language R 3.0.2 was used to
284 determine whether a rate of change was statistically significant. Trends in baseline CO and O₃
285 were reported using SenTheil slopes from the non-parametric Mann–Kendall analysis in ppbv
286 yr⁻¹ with 90 % confidence intervals. Pearson correlation was computed to determine the relation
287 between variables (e.g. baseline CO, baseline O₃, NAO index, relative humidity). The Student t
288 test was conducted to verify statistical significance ($\alpha = 0.10$).

289 To quantify the contribution to a location of interest from biomass burning emissions
290 over an area, we applied the following linear regression models (Wotawa et al., 2001):

$$291 \quad \text{CO} = a_0 + a_1 E \quad (1)$$

292 Where CO is the mixing ratio of baseline CO at each site, E the total CO column over the area, a_0
293 the intercept value, and a_1 the slope value. The combined effect of biomass burning emissions
294 from Russia (E_{Russia}) and Canada (E_{Canada}) was computed using Eq. (2):

$$295 \quad \text{CO} = b_0 + b_1 E_{\text{Russia}} + b_2 E_{\text{Canada}} \quad (2)$$

296 where b_0 , b_1 , and b_2 are regression parameters. Note that E_{Russia} and E_{Canada} were found to be the
297 two emissions sources that contributed significantly to the baseline CO at the seven sites of our
298 study, which is why only these two sources were included in the regression.

299 **3 Results and discussions**

300 **3.1 General characteristics**

301 **3.1.1 Baseline CO**

302 Baseline CO at CS, MWO, PM, TF, and PSP had maxima uniformly in March and
303 minima in varying months over August–October (Fig. 2a and b). Averaged annual maxima were
304 191 ppbv at CS, 180 ppbv at MWO, 155 ppbv at PM, 164 ppbv at TF, and 189 ppbv at PSP over
305 their respective time periods (Table 1). Averaged annual minima were 131 ppbv in August at CS,
306 142 ppbv in September at MWO, 109 ppbv in October at PM, 113 ppbv in August at TF, and 128
307 ppbv in October at PSP. At AI, year-round data were available during 2007–2010, a much
308 shorter time period compared to those at other sites. The seasonal cycles at AI were consistent
309 with other sites, with the average annual maximum 149 ppbv in March and minimum 103 ppbv
310 in September. Previous studies suggested that the annual maximum in cold months resulted from
311 residential heating, vehicle cold starts, and less loss from oxidation by OH, while the annual
312 minimum in fall, instead of in June–July when solar radiation and hence OH concentrations
313 reach annual maxima, was probably the combined effect of biomass burning emissions, mobile
314 combustion emissions, and loss from oxidation by OH (Kopacz et al., 2010; Miller et al., 2008).

315 The annual cycle at WFM was different from those at all other sites, with an annual
316 maximum of 144 ppbv in July and minimum of 103 ppbv in December averaged over January
317 2001–December 2010 (Fig. 2b). To investigate the potential reasons for this different behavior,
318 the data at WFM were compared with those at MWO, a site with slightly higher elevation (2 km
319 a.s.l.) located 208 km to the east (Fig. 1). WFM and MWO are 128 km southwest and 217 km
320 southeast, respectively, from Montreal, the 9th largest city in North America. Over 2001–2009,
321 averaged summertime baseline CO (141 ppbv) at WFM was comparable to that (145 ppbv) at
322 MWO, while averaged wintertime baseline CO (108 ppbv) at WFM was 60 ppbv or 36 % less
323 than that (168 ppbv) at MWO (Fig. 2a and b). This wintertime contrast was probably associated
324 with the large difference between the frequency distributions of wind direction at the two sites.

325 There were 4.7 % of the air masses at WFM from the northeast (22.5–67.5°), compared to 75.4 %
326 of the air masses at MWO from the northwest (247.5–337.5°), the general direction of Montreal.
327 This indicates that MWO was frequently exposed to northwesterly winds carrying air masses
328 potentially influenced by anthropogenic emissions in Montreal, while such influences were rare
329 at WFM. Consequently, much lower baseline CO was found at WFM than at MWO.

330 From April 2001 to December 2010, baseline CO decreased significantly at a rate of -2.5
331 ppbv yr^{-1} at TF, $-4.3 \text{ ppbv yr}^{-1}$ at PSP, and $-2.8 \text{ ppbv yr}^{-1}$ at WFM. Baseline CO decreased at a
332 rate of $-2.3 \text{ ppbv yr}^{-1}$ at MWO over April 2001–March 2009 and $-3.5 \text{ ppbv yr}^{-1}$ at PM over July
333 2004–October 2010 (Table 2). Unlike all other sites, CS exhibited an increasing trend of 2.8
334 ppbv yr^{-1} over April 2001–June 2008. Prior to May 2003, the mixing ratio of baseline CO at CS
335 was similar to that at TF. After May 2003, baseline CO at CS was $\sim 30 \text{ ppbv}$ higher than that at
336 TF and PM (Fig. 2a), resulting in the overall increasing trend. The reasons for such unusually
337 high values at CS are unknown.

338 The U.S. EPA reported a decrease of 52 % in the national average of annual second
339 highest 8 h mixing ratios of CO from 2001 to 2010 (EPA, 2012), corresponding to a rate of -7.8
340 ppbv yr^{-1} (for an decadal average mixing ratio of $\sim 150 \text{ ppbv}$), which was larger than that at any
341 of our sites. Because EPA's trend was estimated using measurements mainly from urban sites
342 with higher concentrations and also focused on the high end of the distribution, it is expected to
343 show larger changes compared to the trend of baseline levels at rural or remote sites from this
344 study, with influence of direct anthropogenic emissions removed.

345 The total CO column from MOPITT retrievals over the eastern US was found to decrease
346 at a rate of $1.4\% \text{ yr}^{-1}$ (or $-2.1 \text{ ppbv yr}^{-1}$ for a decadal average mixing ratio of $\sim 150 \text{ ppbv}$) from
347 2000 to 2011 (Worden et al., 2013), which was comparable to that of the baseline CO in this

348 study. These significant decreasing trends of baseline CO and total column CO were probably
349 associated in large part with anthropogenic CO emissions reductions worldwide (Gratz et al.,
350 2014). Globally, anthropogenic CO emissions showed a slight decrease of $\sim 1\%$ from 1990 to
351 2010 (Granier et al., 2011). In the US and Europe, total anthropogenic CO emissions declined at
352 a rate of $-3\% \text{ yr}^{-1}$ from 2000 to 2010, while increasing trends were found in India ($\sim 1.5\% \text{ yr}^{-1}$)
353 and China ($\sim 3\% \text{ yr}^{-1}$) (Granier et al., 2011). A decreasing trend in CO emissions in China since
354 2005 was suggested by Tohjima et al. (2014) and Zhang et al. (2009).

355 **3.1.2 Baseline O₃**

356 The baseline O₃ concentrations from all sites ranged from 22 ppbv in the fall to 56 ppbv
357 in spring, consistent with baseline levels in the Eastern US that were quantified using a principal
358 component analysis and backward air parcel trajectories by Chan and Vet (2010). The time series
359 of baseline O₃ at all sites showed averaged annual maxima in April and minima in August–
360 October (Fig. 2c and d). Annual maxima averaged over their respective periods at the seven sites
361 occurred all in April and were very close in magnitude, ranging from 47 to 51 ppbv. In
362 comparison, averaged annual minima at the seven sites displayed distinct difference in
363 magnitude and timing, varying over 28–37 ppbv, occurring in August at CS, September at AI
364 and PM, and October at TF, PSP, MWO, and WFM. Studies have suggested that monthly surface
365 O₃ over remote continental areas generally had a spring maximum, attributed to enhanced
366 stratospheric input and hemispheric wide photochemical production (Monks, 2000; Parrish et al.,
367 2013). Here, the fact that baseline CO had annual maxima in spring suggested that the springtime
368 annual maxima of baseline O₃ were possibly associated with photochemical processing of O₃
369 precursors including CO and VOCs that had been built up overwinter on a hemispherical scale
370 (Kopacz et al., 2010; Penkett et al., 1993).

371 A close examination using the Mann–Kendall test suggested no significant trends in
372 baseline O₃ during the study period at all sites (Table 2). Similar results were found in Mace
373 head, Ireland, which is located on the western coast of Europe (Derwent et al., 2007). From 1987
374 to 1997, baseline O₃ at Mace Head had a significant increasing trend of 0.14 ppbv yr⁻¹ followed
375 by a small increase over 1997–1999, and stabilized over 2000–2007 (Derwent et al., 2007).

376 IPCC (2001) suggested that the change of long-term trends in baseline O₃ could be driven
377 by CH₄ oxidation in the presence of NO_x. In a polluted region, O₃ is produced by photochemical
378 reactions of nonmethane hydrocarbons (NMHCs) and NO_x (West et al., 2006). In the global
379 troposphere, CH₄ is the primary anthropogenic VOC (Fiore et al., 2002) and affects global
380 background mixing ratios of O₃ due to its long lifetime (8–9 years). Derwent et al. (2007) found
381 the change of baseline O₃ in Mace Head followed the mixing ratios of baseline CH₄ over 1992–
382 2007. West et al. (2006) found that reducing global anthropogenic CH₄ emissions by 20%
383 beginning in 2010 would reduce O₃ mixing ratios globally by ~ 1 ppbv in 2030. Globally, the
384 growth rate of CH₄ declined from ~ 13 ppbv yr⁻¹ in the early 1980s to near zero over 1999–2006
385 (WMO, 2012). Since 2007, atmospheric CH₄ was increasing again with an average rate of ~ 3
386 ppbv yr⁻¹ (WMO, 2012). These changes in CH₄ mixing ratios can potentially lead to changes in
387 baseline O₃ mixing ratios.

388 On the other hand, global NO_x emissions did not change overall during the study period
389 (Granier et al., 2011). Granier et al. (2011) reported that annual NO_x emissions decreased at a
390 rate of 1.5 Tg yr⁻¹ in western Europe, 0.7 Tg yr⁻¹ in central Europe, ~ 5 Tg yr⁻¹ in the US over
391 2001–2010, while increased at a rate of ~ 5 Tg yr⁻¹ in China and ~ 1.5 Tg yr⁻¹ in India. Xing et
392 al. (2015) found varying trends in NO_x mixing ratios over 1990–2010, with 4.1% in China, -1.4%
393 in the US, and -1.2% in Europe. The annual rates of change in NO_x concentrations were

394 comparable to those in emissions (Xing et al., 2015). This suggests that increasing CH₄ and
395 opposite trends of NO_x emissions worldwide probably contributed to the insignificant trends in
396 baseline O₃ over the northeast US during 2001–2010.

397 **3.2 Seasonal variation of decadal trends in baseline CO and O₃**

398 Generally a decreasing trend was found in baseline CO and no trend in baseline O₃
399 during the decade 2001–2010 as shown in the previous section. However, trends of baseline CO
400 and O₃ were found to vary by season (Table 2). Baseline CO at CS was anomalously high since
401 May 2003 (Fig. 2a) and had increased over the decade in all seasons. As the reasons for the
402 unusually high values at CS are unknown, baseline CO at CS was not included in the subsequent
403 discussion.

404 In spring and winter, baseline CO at PM, TF, and PSP decreased significantly at a rate
405 between -6.5 to -3.7 ppbv yr⁻¹, while no significant decreasing trends were found at the two
406 highest sites MWO and WFM (Table 2). In summer, baseline CO at MWO, PM, TF, and PSP
407 showed decreasing trends varying between -5.5 and -4.3 ppbv yr⁻¹. In fall, baseline CO at all
408 sites decreased significantly at rates varying between -6.4 and -3.2 ppbv yr⁻¹.

409 The overall insignificant change of baseline CO at MWO and WFM in spring and winter
410 could be due to the combined effect of decreasing US emissions and increasing Asian emissions.
411 MWO and WFM are the highest sites situated close to the top of the daytime convective
412 boundary layer, which are more likely impacted by free tropospheric air compared to other sites.
413 Thus, the impact of continental to intercontinental transport could be just as important there, and
414 perhaps at times more important, than regional transport. CO emissions in the US declined at a
415 rate of ~ -3 %yr⁻¹ over 2000–2010, while an overall increasing trend was seen in China over
416 1999–2010, despite a small decrease since 2005 (Granier et al., 2011; Tohjima et al., 2014).

417 Liang et al. (2004), using GEOS-Chem model simulations, found that Asian influence was
418 strongest in spring in the North Pacific lower troposphere, due to the combined effect of efficient
419 ventilation of the Asian boundary layer via midlatitudinal cyclones and convection, long lifetime
420 of CO, and strong springtime biomass burning emissions in southeastern Asia. The same study
421 also found that the Asian influence weakened in summer due to the shorter lifetime of CO and
422 continental export driven most often by convective injection to the upper troposphere, while
423 particularly strong transpacific transport events occurred in spring and winter (Liang et al., 2004).

424 In fall, baseline O₃ did not show significant trends at any of the sites (Table 2). In
425 summer, baseline O₃ showed distinct decreasing trends of -3.1 ppbv yr⁻¹ at AI, -4.7 ppbv yr⁻¹ at
426 both MWO and WFM during their respective time periods, and no trends were found at other
427 sites (Table 2). TF was the only site where baseline O₃ increased significantly at a rate of 2.4
428 ppbv yr⁻¹ in spring and 2.7 ppbv yr⁻¹ in winter over 2001–2010, while other sites showed no
429 trends during the two seasons.

430 Tropospheric O₃ has been changing over the past four decades in response to changes in
431 anthropogenic and natural emissions, stratosphere-tropospheric exchange, pollution transport
432 pathways and O₃ photochemistry (Parrish et al., 2013). Therefore, it was hypothesized that the
433 following factors may have contributed to the significant decreasing trends in summertime
434 baseline O₃ at AI, MWO, WFM and significant increasing trends in springtime and wintertime
435 baseline O₃ at TF:

- 436 1. Decreasing and increasing stratospheric intrusion in summer and winter – spring,
437 respectively;
- 438 2. Decreasing and increasing continental to intercontinental transport of anthropogenic
439 and natural O₃ precursors in summer and winter – spring, respectively;

- 440 3. Decreasing emissions of NO_x from electric power generation and motor vehicles;
441 and
442 4. Changing pollution transport pathways in winter, spring, and summer.

443 Factor #1 was examined using PV data, as one of the physical characteristics of
444 stratospheric air is high value of PV. Time series of PV at 350 K showed no trend in PV over the
445 northeast US during the decade (Fig. 3a). There appeared to be distinct annual cycles in PV with
446 maxima in winter and minima in summer, averaged 1.81×10^{-8} and $1.05 \times 10^{-8} \text{ m}^2\text{s}^{-1}\text{kg}$,
447 respectively (Fig. 3a). Hence, stratospheric intrusion probably had a larger impact on the surface
448 in winter-spring than in summer, which was supported by previous studies (James et al., 2003;
449 Stohl et al., 2003). Such impact would more likely reach higher than lower elevation locations.
450 No trends in baseline O₃ at the two highest sites MWO and WFM appeared to be consistent with
451 what the time series of PV suggested. Moreover, TF, near the sea level (18 m a.s.l.), was less
452 likely influenced by stratospheric intrusion than all other sites. These points were verified using
453 the stratospheric O₃ during 2001–2010 from Liu et al. (2013), which suggested, on seasonal
454 average in the area including all our sites, no contribution to the lowest layer (0.5 km) in summer,
455 or no significant trends in such contribution in winter-spring. Therefore, it seemed unlikely that
456 stratospheric intrusion contributed to the springtime and wintertime increasing trends in baseline
457 O₃ at TF.

458 Significant increases have been reported by Cooper et al. (2012) in springtime and
459 wintertime free tropospheric O₃ over North America, particularly in air masses originating from
460 East Asia. The western US with elevated terrain was much more likely to be influenced by
461 descending free tropospheric air than the eastern US (Cooper et al., 2012). Even if air masses
462 rich in O₃ originating from East Asia reached the US East Coast, they would most likely have a

463 stronger impact on elevated sites. The fact of no trends at any of the elevated sites in spring or
464 winter suggested that long-range transport of O₃ and its precursors from Asia was probably not a
465 cause of increasing springtime and wintertime baseline O₃ at TF (Factor #2).

466 In summer, continental export from East Asia is weaker (Wild and Akimoto, 2001) and
467 Asian emissions have less impact on US surface O₃ relative to domestic emissions than in winter
468 and spring (Reidmiller et al., 2009), which ruled out the effect of long-range transport of Asian
469 emissions on summertime trends in baseline O₃ at our sites. Summer sees the peak of forest fires
470 (Wotawa et al., 2001). Therefore, changes in emissions of CO and other O₃ precursors from
471 biomass burning could influence the trends in summertime baseline O₃ and CO (Sect. 3.3.1).

472 Further analysis suggested that decreasing urban emissions of NO_x quite likely
473 contributed to the rise in springtime and wintertime baseline O₃ at TF (Factor #3). Tropospheric
474 NO₂ column over the US declined by 41% in spring and 33% in summer during the period of
475 1996–2011 (Cooper et al., 2012). Emissions of NO_x in the US were reduced by 48% over 1990–
476 2010, largely due to control of emissions from power plants and mobile sources (Xing et al.,
477 2013). The Northeast US Urban Corridor, extending from Washington D.C. in the south to
478 Boston in the north, was dominated by mobile combustion emissions of NO_x. Annual mixing
479 ratios of NO₂ in New York City decreased at a rate of $-0.3 \text{ ppbv yr}^{-1}$ over 1980–2007 (Buckley
480 and Mitchell, 2011). In winter and early spring with weakened photochemical production,
481 decreased NO_x emissions in urban areas could cause less loss of O₃ via titration by NO (Liu et al.,
482 1987; Jacob et al., 1995; Frost et al., 2006; Jonson et al., 2006), and the result could be enhanced
483 O₃ mixing ratios in urban plumes (Cooper et al., 2010; Wilson et al., 2012). From measurements
484 at our sites, data points of O₃ were selected corresponding to wind from the urban corridor. It
485 was found that the 10th percentile mixing ratio of O₃ at TF in air masses from the urban corridor

486 had been increasing at a rate of $1.81 \text{ ppbv yr}^{-1}$ ($p = 0.05$) in spring and $1.52 \text{ ppbv yr}^{-1}$ ($p < 0.01$)
487 in winter (Fig. 3b and c). This strongly suggests that decreased NO_x emissions in the urban
488 corridor likely had a significant impact on springtime and wintertime baseline O_3 at TF whereas
489 had no similar effects at other sites. In summer with strong photochemistry, decreased emissions
490 of O_3 precursors could lead to reductions in peak summertime O_3 concentrations at surface
491 continental sites (Cooper et al., 2012; Parrish et al., 2013). No significant change was found in
492 summertime 10th percentile mixing ratios of O_3 in air masses from the urban corridor at TF,
493 which was consistent with the relatively constant summertime baseline O_3 at TF as
494 aforementioned.

495 The implementation of the Acid Rain Program and the NO_x Budget Trading Program
496 (NBP) also reduced NO_x emissions from the power plants (Xing et al., 2013). In the Ohio River
497 Valley, where power plants dominate, both NO_2 column and NO_x emissions decreased by 38 and
498 34% over 1999–2005 (Kim et al., 2006). However, the 10th percentile mixing ratio of O_3 in air
499 masses from the southwest did not show any significant change in winter, spring, and summer at
500 PSP, which is located to the northeast of the Ohio River Valley (Fig. 3b–d).

501 There is interannual variability in transport pathways, temperature, water vapor, solar
502 radiation, and natural emissions (e.g., lightning, forest fires, and vegetation). A close
503 examination of the NOAA CRN data revealed that springtime solar radiation at TF was
504 increasing at a rate of $24.5 \text{ W m}^{-2} \text{ yr}^{-1}$ ($p = 0.03$) over 2002–2010, with the lowest value of 432
505 Wm^{-2} in 2002 (Fig. 3a), while no significant trend was found in winter. Without the value in
506 spring 2002, the solar radiation flux at TF increased at a rate of $9.4 \text{ W m}^{-2} \text{ yr}^{-1}$ in spring ($p =$
507 0.02). This trend in springtime solar radiation at TF was possibly related to cloudiness in
508 response to changing cyclone activity associated with varying atmospheric circulation, which

509 could have affected baseline O₃. More frequent cyclone activities, wetter conditions associated
510 with the North Atlantic storm track parallel to the eastern US coast could be possible factors
511 leading to the very low solar radiation flux in spring 2002. Further research is warranted to fully
512 understand what may have caused this phenomenon. The impact of changes in weather
513 conditions and large scale circulation on baseline O₃ was further explored in the following
514 section.

515 **3.3 Factors controlling baseline CO and O₃ in spring and summer**

516 This section further identifies factors impacting the variation of baseline CO and O₃.
517 Emphasis was placed on spring and summer, when there are strong intercontinental transport and
518 photochemistry involving O₃ and CO (Cooper et al., 2010; Emmons et al., 2003), as well as
519 exceedances of NAAQS.

520 **3.3.1 Impact of wildfires in summer**

521 Large interannual variability in global CO mixing ratios was attributed to variations in
522 biomass burning emissions (Novelli et al., 2003; Wotawa et al., 2001). Studies (Hecobian et al.,
523 2011; Oltmans et al., 2010) suggested that biomass burning effluents from Russia and Canada
524 flowed into North America. In addition, California and Alaska were two US states with
525 considerable fire emissions of CO, which reportedly impacted the air quality over North America
526 (McKendry et al., 2011; Real et al., 2007).

527 Fire emissions of CO in summer were estimated using the GFED dataset and MOPITT
528 retrievals (Fig. 4a and b). The GFED data suggested that massive wildfires occurred in Russia in
529 2002, 2003, and 2008 with annual CO emissions of 42.1, 71.1, and 35.8 Tg, respectively. Annual
530 fire emissions from Canada were 17.4 Tg in 2004 and 18.3 Tg in 2010. In Alaska, the largest
531 fires occurred in 2004 with 13.1 Tg CO emitted, while in California the largest fire emissions of

532 CO were 1.3 Tg in 2008. From 2001 to 2010, the total CO emissions from wildfires in Russia,
533 Canada, Alaska and California varied from 19.9 to 84.3 Tg, with the lowest and the highest in
534 2007 and 2003, respectively.

535 To quantify contributions of wildfires from these four areas to summertime baseline CO
536 levels at our sites, a linear regression model was used together with MOPITT total CO column
537 retrievals. Monthly CO columns were first correlated with monthly GFED fire emissions of CO
538 for the four areas. The correlation coefficients were 0.89, 0.81, 0.81, and 0.84 ($p < 0.01$ for the
539 four values) for Russia, Canada, California, and Alaska, respectively, suggesting that the
540 variability in total column CO over those areas was dominated by that of fire emissions.

541 Further, it was found that the contributions of fire emissions from Russia and Canada to
542 the variability of summertime baseline CO at the 56 sites were averaged to be 37% and 22%,
543 respectively (Table 3), and their combined contribution was averaged to be 41%. Contributions
544 from Alaska and California were negligible at these six sites. Globally, there is approximately 1
545 billion ha closed forest in the boreal region, about two thirds of which is situated in Russia
546 (Harden et al., 2000). CO emissions from wildfires in Russia and Canada contributed 49.5 and
547 29.6%, respectively, to the total CO emissions from wildfires in Northern Hemispheric
548 midlatitudes (30–90°N). Understandably, baseline CO was well correlated to wildfires in Russia
549 and Canada at most sites except at PSP.

550 The insignificant correlation between baseline CO at PSP and wildfires emissions from
551 Russia and Canada was possibly due to less dynamical circulation at the site. PSP had the lowest
552 wind speed of 0.47 m s^{-1} amongst all sites based on surface wind speed averaged over summers
553 of 2001–2010 (Fig. 5a). This appeared to be consistent with the position of PSP relative to the
554 pressure systems throughout the year (Fig. 5b–e). The climatological seasonal maps of sea level

555 pressure suggest that PSP is located either on the periphery of the subtropical high in summer –
556 fall, or the periphery of the North American trough, where wind tends to be the weakest. In
557 comparison, other sites are either located at the top of the boundary layer, and/or tend to be
558 positioned within the North American trough, more directly under the influence of the westerly
559 wind often facilitating global transport.

560 Since wildfires provide a substantial source of NO_x and hydrocarbons, O_3 is expected to
561 form in fire plumes. Some of these air pollutants live long enough to travel over long distances,
562 which could elevate baseline O_3 globally (Jaffe et al., 2004). Corresponding to the largest fire
563 emissions in summer 2003 in Russia (Fig. 4a), baseline CO in that season at all sites reached the
564 decadal maxima, and baseline O_3 was the highest of all summers at AI, CS, MWO, TF, and
565 WFM (Fig. 4c and d). Jaffe et al. (2004) also suggested that emissions from Siberia forest fires in
566 summer 2003 were transported to North America resulting in enhancements of 23–37 and 5–9
567 ppbv in summertime baseline CO and O_3 , respectively, at 10 sites in Alaska, Canada, and the
568 Pacific Northwest.

569 The second largest summertime baseline CO mixing ratio of the decade was found in
570 summer 2004 at ~~CS~~, TF, and WFM (Fig. 4c), although the total CO emissions from wildfires in
571 Russia and Canada during that season was 20.4 Tg, 16% smaller than 24.4 Tg, the decadal
572 (2001–2010) average annual CO emissions from the two countries. Over Alaska, the
573 geopotential height in summer 2004 was ~ 40 gpm higher than normal years (Fig. 6a–c). This
574 relatively higher pressure field led to drier and warmer conditions over Alaska and southwestern
575 Canada with 82% relative humidity and 12°C surface temperature, the driest and warmest of the
576 decade (Fig. 6d). Such weather conditions are conducive to occurrence of wildfires. In summer
577 2004, CO emissions from wildfires in Canada and Alaska contributed 48.5 and 36.5%,

578 respectively, to the Northern Hemispheric total, compared to the decadal (2001–2010) average
579 contributions of 49.5, 10.6, and 29.6% from Russia, Alaska, and Canada, respectively.
580 Correspondingly, the 13.1 Tg CO emissions from wildfires in Alaska were the largest over the
581 decade, and the 17.4 Tg CO emissions from wildfires in Canada were the second largest of the
582 decade, following the largest in summer 2010 (Fig. 4a). On the other hand, the streamlines over
583 Canada suggested an unusually strong northeasterly component in summer 2004. The high
584 pressure system over Alaska and southwestern Canada most likely strengthened the westward
585 transport of wildfires effluents from Alaska and Canada (Fig. 6c). The combination of these two
586 factors resulted in efficient transport of massive CO emissions from fires over Alaska and
587 Canada. Smoke from these fires over the continental United States was observed in satellite
588 images of aerosol optical depth (AOD) from the GOES (Geostationary Operational
589 Environmental Satellites) (Kondragunta et al., 2008) and MODIS (Moderate Resolution Imaging
590 Spectro-radiometer) aboard Terra (Mathur, 2008), and extensive plumes of enhanced CO
591 concentrations were captured in MOPITT (Measurements of Pollutants in the Troposphere)
592 retrievals (Pfister et al., 2005).

593 Mann–Kendall trend analysis indicated no significant decreasing trends in biomass
594 burning emissions from Alaska, Canada, and California. In contrast, CO emissions from
595 wildfires in Russia decreased at a rate of -0.51 Tg yr^{-1} ($p = 0.10$). Summertime baseline CO at
596 MWO, PM, TF, and PSP decreased at a rate between -5.5 and $-4.3 \text{ ppbv yr}^{-1}$ and baseline O₃ at
597 AI, MWO, and WFM decreased at a rate between -4.7 and $-3.1 \text{ ppbv yr}^{-1}$ (Sect. 3.2). Based on
598 regression analysis, as a result of a 0.51 Tg yr^{-1} decrease in CO emissions from wildfires in
599 Russia, baseline O₃ decreased by 0.04 – $0.07 \text{ ppbv yr}^{-1}$ ($p = 0.08$ – 0.10) at AI, MWO, WFM, and
600 CS, while baseline CO declined by 0.14 – $0.22 \text{ ppbv yr}^{-1}$ ($p = 0.01$ – 0.10) at AI, TF, MWO, and

601 WFM. Hence, the decreasing trend of biomass burning emissions in Russia was likely a major
602 factor causing the decreasing trends in baseline CO and O₃ in summer at our sites.

603 **3.3.2 Impact of cyclone activity and AO in summer**

604 Meteorology is another factor that can influence summertime baseline CO and O₃ across
605 the northeast US over 2001–2010. Of all the meteorological variables, midlatitude cyclone
606 frequency is an important one that can impact regional air quality greatly. It affects not only
607 boundary layer ventilation, humidity, solar radiation, and temperature but also general circulation
608 of the regional atmosphere (Leibensperger et al., 2008).

609 Time series of summertime counts of cyclones in the northeast US showed strong
610 interannual variability (Fig. 7a). The counts of cyclones in 2003, 2006, 2008, 2009, and 2010
611 were greater than 12, the average of summer 2001–2010. Summer 2009 experienced the largest
612 number of cyclones (20) passing the northeast US during the 2001–2010 period. Other summers
613 experienced below-average cyclones. No overall trend was found in the counts of cyclones
614 during the study period. Our calculated numbers of cyclones were consistent with the results for
615 the same years from Leibensperger et al. (2008) and Bauer and Del Genio (2006).

616 In summer, cyclones tend to move around the 500 hPa vortex, which is over the cold
617 Arctic Ocean with broadly symmetric flow around it (Serreze et al., 2007). On the North
618 American side, the high latitude flow on the 500 hPa pressure level has a southward component,
619 which tends to steer systems away from the Arctic Ocean (Fig. 7b). Composite analyses
620 associated with years of strong (2003, 2006, 2008, 2009, and 2010) vs. weak (2001, 2002, 2004,
621 2005, and 2007) cyclone activities revealed distinct differences in regional to large scale
622 circulation (Fig. 7c). There turned out to be a pronounced positive difference of ~ 35 gpm
623 centered over Baffin Island (north of the northeast US) and a negative difference of ~ 25 gpm

624 centered over the northeast US (Fig. 7c). This difference was related to the negative phase of AO
625 (Fig. 7a), when surface pressure is abnormally high in the polar region and low in the
626 midlatitudes (Archambault et al., 2008). In a negative AO season, Arctic lows and westerlies are
627 weaker, leading to more frequent cold-air outbreaks down to Eurasia and the US, and stormy
628 weather over the Mediterranean (Hess and Lamarque, 2007), and ultimately low baseline CO and
629 O₃ across the northeast US.

630 A case in point was summer 2009 with the largest cyclone count (20) and the strongest
631 negative AO phase (-0.92) of the decade (Fig. 7a). Consistent with earlier results, the difference
632 of 500 hPa geopotential height between summer 2009 and the 10 year average had negative
633 anomalies up to ~ -60 gpm over the North American continent and positive anomalies up to ~
634 65 gpm centered near the pole (Fig. 7d). The sea level pressure field (Fig. 7e) featured a
635 pronounced mean low over southern Canada and the streamlines suggested an unusually strong
636 northeasterly component. Indeed, the frequency distribution of wind direction at each site
637 suggested more frequent occurrence of northeasterly wind (22.5–112.5°), with 21% at PM, 9% at
638 MWO, 42% at TF, 11% at PSP, and 13% at WFM (Fig. 8). In summer 2009, the northeast US
639 was more often under the influence of cold frontal passages associated with the largest number
640 of cyclones passing through the region. As a result, the northeast US was exposed most
641 frequently to air masses of Arctic origin. Moreover, emissions from large scale wildfires clearly
642 had global effects as discussed in Sect. 3.3.1. In summer 2009, ~ 11.9 Tg CO, the lowest of the
643 decade, was emitted from wildfires in Russia and Canada (Fig. 7f). Hence, the lowest fire
644 emissions of CO and the most frequent cyclone activities were likely two important factors
645 leading to the lowest summertime baseline CO and O₃ in 2009 at the study sites.

646 A contrasting case was summer 2003, when AO was negative and 15 cyclones passed the
647 region (Fig. 7a), 25% greater than the decadal mean (12), and yet baseline CO and O₃ at the sites
648 reached the decadal maxima (Figs. 4c, d and 7f). According to the analysis above, baseline CO
649 and baseline O₃ were expected to be lower during this summer than the decadal average as a
650 result of above-average passages of cyclones. However, in summer 2003 CO emissions from
651 Russian and Canadian wildfires were the largest of the decade (Sect. 3.3.1), counteracting the
652 effect of the AO. Another interesting example was summer 2007 which had the lowest cyclone
653 activity of the decade (Fig. 7a), and the total CO emissions from wildfires in Russia and Canada
654 were 13.6 Tg, the second lowest of the decade following summer 2009 (Fig. 7f). The site-
655 average baseline CO and O₃ levels in summer 2007 were below the decadal means. Therefore,
656 the effect of biomass burning may dominate over that of AO and cyclone activity during some
657 summers, while the two worked in concert during others.

658 Overall, no distinct correlation between counts of cyclones and baseline O₃ was found at
659 most sites (AI, CS, MWO, PM, TF, WFM), while no significant correlation between counts of
660 cyclones and baseline CO was found at any of the sites. The only exception was PSP where the
661 count of cyclones was found to be reasonably anti-correlated with baseline O₃ ($r = -0.56$, $p =$
662 0.05) in the summer. As discussed in Sect. 3.3.1, PSP was the only site that did not seem to be
663 affected by the Russian and Canadian wildfire emissions as all other sites were, possibly due to
664 its being situated in a region less impacted by large-scale dynamics. Perhaps this very dynamic
665 characteristic cast the site under a predominant influence of synoptic systems, e.g., the Bermuda
666 High and cold frontal passages. As commonly known, high mixing ratios of O₃ in the northeast
667 occur under summertime stagnant, clear sky conditions associated with the Bermuda High
668 (Logan, 1989; Vukovich, 1995; Hegarty et al., 2007; Lai et al., 2012), while low O₃ was often

669 linked to cold fronts which sweep out polluted air leaving much cooler and cleaner air in the
670 northeast (Cooper et al., 2001; Leibensperger et al., 2008; Li et al., 2005). Conceivably, with
671 more frequent cyclones passing the northeast US, lower concentrations of baseline CO and O₃
672 would be expected, and the predominant effect of such synoptic systems could quite likely lead
673 to anticorrelation between the baseline CO/O₃ levels and cyclone activities.

674 3.3.3 Impact of NAO in spring (March and April)

675 Wildfires in March and April were scarce, with mean CO emissions of 1.78 Tg in Russia
676 and 0.004 Tg in Canada over 2001–2010, negligible compared to emissions during the fire
677 season (May–September). To focus on the impact of large circulation patterns on baseline CO
678 and O₃ in spring, the May data were excluded to avoid the effect of biomass burning. Springtime
679 baseline O₃ at each site showed strong and consistent interannual variation up to 10 ppbv (Fig.
680 9a). The baseline O₃ mixing ratio averaged at all the seven sites over the decade was 46.5 ppbv,
681 and exceeded the average (>46.5 ppbv) in 2001, 2003, 2005, 2008, 2010, and was below average
682 (≤ 46.5 ppbv) in 2002, 2004, 2006, 2007, 2009 (Fig. 9a).

683 The difference of 850 hPa geopotential height between the lower and higher O₃ years is
684 shown in Fig. 10. There was a pronounced difference up to 40 gpm in the Bermuda/Azores high
685 and ~ -40 gpm in the Icelandic low, which resulted in stronger gradient flow between the two
686 pressure systems ~~and was indicative of the positive phase of NAO, known as the positive phase~~
687 ~~of NAO~~. Over 2001–2010, NAO index was significantly positive in 2002, 2004, 2007, 2009 and
688 negative in 2001, 2005, 2008, 2010, which corresponded mostly to the years of below and above
689 the decadal average baseline O₃, respectively. Significant negative correlation was found between
690 the NAO index and baseline O₃ at each site (Table 4) (~~CS: $r = -0.75$, $p = 0.03$; MWO: $r = -0.68$,~~
691 ~~$p = 0.03$; PM: $r = -0.81$, $p = 0.03$; TF: $r = -0.81$, $p < 0.01$; PSP: $r = -0.58$, $p = 0.06$; WFM: $r =$~~

692 | ~~$-0.51, p = 0.10$~~ . The negative correlation between baseline O₃ and the NAO index could be a
693 | result of multiple factors, such as solar flux, stratosphere-tropospheric exchange, and continental
694 | export of O₃ produced in North America. ~~It should be noted that, no significant correlation was~~
695 | ~~found between the NAO index and baseline CO at any of the sites, which suggests that NAO is~~
696 | ~~not linked to or played an insignificant role in the interannual variability of baseline CO.~~

697 | The first possible explanation for the baseline O₃ and NAO index anticorrelation was
698 | changes in surface solar radiation flux during positive/negative NAO years. During a positive
699 | NAO year, the mean North Atlantic storm track parallels the eastern North American coastline
700 | before extending northeastward to near Iceland (Rogers, 1997). This storm track and its
701 | associated moisture transport and convergence lead to relatively wet conditions near the eastern
702 | US coast (Archambault et al., 2008; Hurrell, 1995). During a negative NAO year, the mean
703 | North Atlantic storm track is more zonal (Rogers, 1997), leading to relatively dry conditions near
704 | the eastern US coast (Archambault et al., 2008; Hurrell, 1995). At ~~our coastal~~ sites around the
705 | northeast US coast (CS and TF), significant correlation was found between relative humidity and
706 | the NAO index (~~CS: $r = 0.85, p = 0.02$; TF: $r = 0.64, p = 0.06$~~), while the correlation was weaker
707 | at inland, elevated sites (PSP and WFM) (~~PSP: $r = 0.23, p = 0.26$; WFM: $r = 0.40, p = 0.13$~~)
708 | (Table 4 and Fig. 9b).

709 | During positive NAO years, wetter conditions indicate higher relative humidity and more
710 | cloudiness, most likely leading to reduced solar radiation flux near the surface and subsequently
711 | less O₃ production. As expected, a significant negative correlation was found between relative
712 | humidity and solar radiation (~~$r = -0.67, p = 0.05$~~) (~~Fig. 9b~~) and a significant positive correlation
713 | between baseline O₃ and solar radiation flux (~~$r = 0.75, p = 0.03$~~) at TF in March and April (Table
714 | 4 and Fig. 9b). No significant correlation between these variables was found in other seasons.

715 Another possible explanation for the negative correlation between NAO index and
716 baseline O₃ was the influence of stratospheric intrusion. Dynamically, the North American
717 trough induces descending air on its tailing side and in the upper troposphere it can cause
718 tropopause folding with stratospheric air mixing downward into the troposphere. The difference
719 of the PV patterns between positive NAO years and negative NAO years is illustrated in Fig. 11.
720 Negative anomalies of $\sim -0.6 \times 10^{-9} \text{ m}^2 \text{ s}^{-1} \text{ kg}$ were found over the northeast US, suggesting that
721 positive NAO was related to less stratospheric intrusion (Hess and Lamarque, 2007) over the
722 northeast US. This is consistent with lower baseline O₃ levels during positive NAO springs. This
723 was further verified using the stratospheric O₃ dataset constructed by Liu et al. (2013).
724 Stratospheric O₃ was hardly detected at the lowest two layers (i.e., 0.5 and 1.5 km) in April. In
725 March, $\sim 40\text{--}60$ ppbv of stratospheric O₃ reached the lowest layer in our study area in 2004 and
726 2006–2008 and reached the 1.5 km layer in 2001–2008. The stratospheric contribution to the 0.5
727 km layer was the largest in March 2008, when NAO was negative (Fig. 9).

728 The third possible factor affecting baseline O₃ over the northeast US was the effect of
729 North American continental export. During a positive NAO phase, the anticyclonic circulation
730 off the US east coast and the cyclonic circulation across the North Atlantic were amplified with a
731 northward shift (Rogers, 1997). As a result, stronger surface wind was found near 50°N across
732 the North Atlantic basin and into Northern Europe (Hess and Lamarque, 2007). Annual wind
733 speed from the west (247.5–337.5°) was calculated at the study sites (Fig. 9c). Positive
734 correlation was found between surface wind and NAO index at [MWO, CS, and TF \(Table 4\)](#)
735 [most sites \(MWO: \$r = 0.76, p = 0.02\$; CS: \$r = 0.68, p = 0.06\$; TF: \$r = 0.57, p = 0.09\$ \)](#). Eckhardt et
736 al. (2004) found that the warm conveyor belt over the northeast US coast occurred $\sim 12\%$ more
737 frequently in positive NAO years than in negative NAO years. The ending trajectories of the

738 warm conveyor belt in positive NAO years extended further eastward into western and northern
739 Europe (Eckhardt et al., 2004). It was suggested that in a positive NAO year, the O₃ produced
740 over the northeast US was less likely accumulated in the region, and was more likely transported
741 faster off the continent and across the Atlantic Ocean. These changes were consistent with the
742 positive anomalies of O₃ observed over northwestern Europe (Christoudias et al., 2012; Eckhardt
743 et al., 2003). Negative correlation, although insignificant, was also found between baseline CO
744 and the NAO index at most of our study sites (Table 4). North American continental export
745 could also impact the variation of baseline CO, while this impact could be confounded by other
746 factors, e.g. stratospheric intrusion. Specifically, during positive NAO years, more continental
747 outflows lead to a decrease in baseline CO, while less stratospheric intrusion would lead to less
748 dilution of surface CO and thus increase baseline CO levels. Further research is warranted to
749 fully understand the relationship between baseline CO and NAO.

750 **4 Summary**

751 Baseline CO and O₃ at seven rural sites in the northeast US were examined for their
752 seasonal and interannual variabilities during the time period of 2001–2010, and potential
753 mechanisms controlling the variabilities were investigated. It was found that baseline CO at most
754 sites (MWO, PM, TF, PSP, and WFM) decreased significantly at a rate between –4.3 to –2.3
755 ppbv yr⁻¹, while baseline O₃ was relatively constant. No trends were found in baseline O₃ at all
756 sites probably resulting from relatively constant mixing ratios of CH₄ in the 2000s and opposite
757 rates of change in NO_x emissions around the world.

758 In spring and winter, baseline CO at MWO and WFM did not exhibit a significant trend,
759 possibly a result of the combined effect of decreasing emissions in the northeast US and
760 increasing emissions in Asia. TF, a coastal rural site, was the only location where baseline O₃

761 was found to increase significantly at a rate of 2.4 and 2.7 ppbv yr⁻¹ in spring and winter,
762 respectively, most likely caused by the decrease in NO_x emissions over the urban corridor.

763 It was found that interannual variations of baseline CO and O₃ were predominantly
764 influenced by biomass burning emissions, cyclone activities, and NAO. In summer, ~ 38% of
765 baseline CO variability was attributed to CO emissions from forest fires in Russia and ~ 22% to
766 emissions from forest fires in Canada. The lowest mixing ratios of baseline CO and O₃ at most
767 sites in summer 2009 were linked to frequent cyclone activity, which were induced by the
768 unusually weak low pressure system in the Arctic region. In spring, a significant negative
769 correlation was found between baseline O₃ and the NAO index, potentially due to variations of
770 solar flux, stratospheric intrusion, and continental export.

771 On 1 October 2015 the U.S. EPA lowered the NAAQS for ground-level O₃ to 70 ppbv ~~In~~
772 ~~December 2014, the U.S. EPA proposed to tighten the 2008 NAAQS for daily maximum 8 h~~
773 ~~average O₃ from 75 ppbv to a level within a range of 65–70 ppbv to provide to improve~~
774 protection of public health and welfare (EPA, 2014) ([http://www3.epa.gov/ozonepollution/pdfs/](http://www3.epa.gov/ozonepollution/pdfs/20151001overviewfs.pdf)
775 [20151001overviewfs.pdf](http://www3.epa.gov/ozonepollution/pdfs/20151001overviewfs.pdf)). As the O₃ NAAQS are set closer to background levels, states will face
776 ever increasing challenges with regard to fulfilling their obligation for NAAQS attainment.
777 Through this study it was reinforced that, in addition to domestic emission control,
778 intercontinental transport of anthropogenic emissions and wildfires emissions together with
779 meteorological conditions should be considered for an encompassing, cost-effective emission
780 control strategy that accounts for impacts of regional to global emissions and moreover
781 emissions of multi-pollutants (e.g., CO, CH₄, NO_x, and NMHCs). In addition, the relationships
782 between baseline O₃/CO and various factors (e.g. NO_x emission controls, biomass burning
783 emissions, NAO, and AO) examined in this study can also be used as reference point for

784 evaluating global/regional air quality modeling systems that are used in air quality management
785 applications. One limitation of this study is that it was based on ten-year observations, and hence
786 it was unlikely to predict the potential changes in natural emissions and AO/NAO signals as well
787 as their impacts on baseline O₃. Future research is warranted to further address the issues
788 identified in this work on climatological time scales.

789 *Acknowledgements.* This work was funded by the Environment Protection Agency grant
790 #83521501. We are grateful to Z. Ye, Y. Zhang, R. D. Yanai, G. Townsend, and E. P. Law for
791 their valuable suggestions and help. We thank K. Cochrane and K. Yan for their assistance in the
792 early stage of the study.

793 *Disclaimer.* Although this work has been reviewed and approved for publication by the U.S.
794 Environmental Protection Agency (EPA), it does not reflect the views and policies of the agency.

795

796 **References**

797 Archambault, H. M., Bosart, L. F., Keyser, D., and Aiyyer, A. R.: Influence of large-scale flow
798 regimes on cool-season precipitation in the northeastern United States, *Mon. Weather Rev.*, 136,
799 2945–2963, doi:10.1175/2007MWR2308.1, 2008.

800 Bae, M. S., Schwab, J. J., Chen, W. N., Lin, C. Y., Rattigan, O. V., and Demerjian, K. L.:
801 Identifying pollutant source directions using multiple analysis methods at a rural location in New
802 York, *Atmos. Environ.*, 45, 2531–2540, doi:10.1016/j.atmosenv.2011.02.020, 2011.

803 Barnston, A. G. and Livezey, R. E.: Classification, seasonality and persistence of low-frequency
804 atmospheric circulation patterns, *Mon. Weather Rev.*, 115, 1083–1126, 1987.

805 Bauer, M. and Del Genio, A. D.: Composite analysis of winter cyclones in a GCM: influence on
806 climatological humidity, *J. Climate*, 19, 1652–1672, doi:10.1175/JCLI3690.1, 2006.

807 Bell, M. L., Goldberg, R., Hogrefe, C., Kinney, P. L., Knowlton, K., Lynn, B., Rosenthal, J.,
808 Rosenzweig, C., and Patz, J. A.: Climate change, ambient ozone, and health in 50 US cities,
809 *Clim. Change*, 82, 61–76, doi:10.1007/s10584-006-9166-7, 2007.

810 Brand, S., Dethloff, K., and Handorf, D.: Tropospheric circulation sensitivity to an interactive
811 stratospheric ozone, *Geophys. Res. Lett.*, 35, 1–5, doi:10.1029/2007GL032312, 2008.

812 Brandt, R. E., Schwab, J. J., Casson, P. W., Roychowdhury, U. K., Wolfe, D., Demerjian, K. L.,
813 Civerolo, K. L., Rattigan, O. V., and Felton, H. D.: Atmospheric chemistry measurements at
814 Whiteface Mountain, NY: ozone and reactive trace gases, *Aerosol and Air Quality Research*,
815 submitted to special issue, 2015.

816 Buckley, S. M. and Mitchell, M. J.: Improvements in urban air quality: case studies from New
817 York state, USA, *Water Air Soil Poll.*, 214, 93–106, doi:10.1007/s11270-010-0407-z, 2011.

818 Chan, E.: Regional ground-level ozone trends in the context of meteorological influences across
819 Canada and the eastern United States from 1997 to 2006, *J. Geophys. Res.-Atmos.*, 114, 1–18,
820 doi:10.1029/2008JD010090, 2009.

821 Chan, E. and Vet, R. J.: Baseline levels and trends of ground level ozone in Canada and the
822 United States, *Atmos. Chem. Phys.*, 10, 8629–8647, doi:10.5194/acp-10-8629-2010, 2010.

823 Christoudias, T., Pozzer, A., and Lelieveld, J.: Influence of the North Atlantic Oscillation on air
824 pollution transport, *Atmos. Chem. Phys.*, 12, 869–877, doi:10.5194/acp-12-869-2012, 2012.

825 Cooper, O. R., Moody, J. L., Parrish, D. D., Trainer, M., Ryerson, T. B., Holloway, J. S., Hübler,
826 G., Fehsenfeld, F. C., Oltmans, S. J., and Evans, M. J.: Trace gas signatures of the airstreams
827 within North Atlantic cyclones: case studies from the North Atlantic Regional Experiment
828 (NARE '97) aircraft intensive, *J. Geophys. Res.-Atmos.*, 106, 5437–5456,
829 doi:10.1029/2000JD900574, 2001.

830 Cooper, O. R., Parrish, D. D., Stohl, A., Trainer, M., Nédélec, P., Thouret, V., Cammas, J. P.,
831 Oltmans, S. J., Johnson, B. J., Tarasick, D., Leblanc, T., McDermid, I. S., Jaffe, D., Gao, R.,
832 Stith, J., Ryerson, T., Aikin, K., Campos, T., Weinheimer, A., and Avery, M. A.: Increasing
833 springtime ozone mixing ratios in the free troposphere over western North America, *Nature*, 463,
834 344–348, doi:10.1038/nature08708, 2010.

835 Cooper, O. R., Gao, R. S., Tarasick, D., Leblanc, T., and Sweeney, C.: Long-term ozone trends
836 at rural ozone monitoring sites across the United States, 1990–2010, *J. Geophys. Res.-Atmos.*,
837 117, 1990–2010, doi:10.1029/2012JD018261, 2012.

838 Creilson, J. K., Fishman, J., and Wozniak, A. E.: Intercontinental transport of tropospheric ozone:
839 a study of its seasonal variability across the North Atlantic utilizing tropospheric ozone residuals
840 and its relationship to the North Atlantic Oscillation, *Atmos. Chem. Phys.*, 3, 2053–2066,
841 doi:10.5194/acp-3-2053-2003, 2003.

842 Creilson, J. K., Fishman, J., and Wozniak, A. E.: Arctic oscillation-induced variability in
843 satellitederived tropospheric ozone, *Geophys. Res. Lett.*, 32, 1–5,
844 doi:10.1029/2005GL023016, 2005.

845 Cui, J., Pandey Deolal, S., Sprenger, M., Henne, S., Staehelin, J., Steinbacher, M., and Nédélec,
846 P.: Free tropospheric ozone changes over Europe as observed at Jungfraujoch (1990–2008): an
847 analysis based on backward trajectories, *J. Geophys. Res.-Atmos.*, 116, 1–14,
848 doi:10.1029/2010JD015154, 2011.

849 Daniel, J. S. and Solomon, S.: On the climate forcing of carbon monoxide, *J. Geophys. Res.*
850 *Atmos.*, 103, 13249–13260, doi:10.1029/98JD00822, 1998.

851 Derwent, R. G., Simmonds, P. G., Manning, A. J., and Spain, T. G.: Trends over a 20-year
852 period from 1987 to 2007 in surface ozone at the atmospheric research station, Mace Head,
853 Ireland, *Atmos. Environ.*, 41, 9091–9098, doi:10.1016/j.atmosenv.2007.08.008, 2007.

854 Duncan, B. N. and Bey, I.: A modeling study of the export pathways of pollution from Europe:
855 seasonal and interannual variations (1987–1997), *J. Geophys. Res.-Atmos.*, 109, D08301,
856 doi:10.1029/2003JD004079, 2004.

857 Dutkiewicz, V. A., Husain, L., Roychowdhury, U. K., and Demerjian, K. L.: Impact of Canadian
858 wildfire smoke on air quality at two rural sites in NY state, *Atmos. Environ.*, 45, 2028–
859 2033, doi:10.1016/j.atmosenv.2011.01.072, 2011.

860 Eckhardt, S., Stohl, A., Beirle, S., Spichtinger, N., James, P., Forster, C., Junker, C., Wagner, T.,
861 Platt, U., and Jennings, S. G.: The North Atlantic Oscillation controls air pollution transport to
862 the Arctic, *Atmos. Chem. Phys.*, 3, 1769–1778, doi:10.5194/acp-3-1769-2003, 2003.

863 Eckhardt, S., Stohl, A., Wernli, H., James, P., Forster, C., and Spichtinger, N.: A 15-year
864 climatology of warm conveyor belts, *J. Climate*, 17, 218–237, 2004.

865 Emmons, L. K., Hess, P., Klonecki, A., Tie, X., Horowitz, L., Lamarque, J.-F., Kinnison, D.,
866 Brasseur, G., Atlas, E., Browell, E., Cantrell, C., Eisele, F., Mauldin, R. L., Merrill, J., Ridley, B.,
867 and Shetter, R.: Budget of tropospheric ozone during TOPSE from two chemical transport
868 models, *J. Geophys. Res.-Atmos.*, 108, 8372, doi:10.1029/2002JD002665, 2003.

869 Fiore, A. M., Jacob, D. J., Bey, I., Yantosca, R. M., Field, B. D., Fusco, A. C., and Wilkinson, J.
870 G.: Background ozone over the United States in summer: origin, trend, and contribution to
871 pollution episodes, *J. Geophys. Res.-Atmos.*, 107, ACH 11-1–ACH 11-25,
872 doi:10.1029/2001JD000982, 2002.

873 Frost, G. J., McKeen, S. A., Trainer, M., Ryerson, T. B., Neuman, J. A., Roberts, J. M., Swanson,
874 A., Holloway, J. S., Sueper, D. T., Fortin, T., Parrish, D. D., Fehsenfeld, F. C., Flocke, F.,
875 Peckham, S. E., Grell, G. A., Kowal, D., Cartwright, J., Auerbach, N., and Habermann,
876 T.: Effects of changing power plant NO_x emissions on ozone in the eastern United States: proof
877 of concept, *J. Geophys. Res.-Atmos.*, 111, D12306, doi:10.1029/2005JD006354, 2006.

878 Granier, C., Bessagnet, B., Bond, T., D'Angiola, A., van der Gon, H. D., Frost, G. J., Heil, A.,
879 Kaiser, J. W., Kinne, S., Klimont, Z., Kloster, S., Lamarque, J. F., Liousse, C., Masui, T., Meleux,
880 F., Mieville, A., Ohara, T., Raut, J. C., Riahi, K., Schultz, M. G., Smith, S. J., Thompson, A., van
881 Aardenne, J., van der Werf, G. R., and van Vuuren, D. P.: Evolution of anthropogenic and
882 biomass burning emissions of air pollutants at global and regional scales during the 1980–2010
883 period, *Clim. Change*, 109, 163–190, doi:10.1007/s10584-011-0154-1, 2011.

884 Gratz, L. E., Jaffe, D. A., and Hee, J. R.: Causes of increasing ozone and decreasing carbon
885 monoxide in springtime at the Mt. Bachelor Observatory from 2004 to 2013, *Atmos. Environ.*,
886 109, 323–330, doi:10.1016/j.atmosenv.2014.05.076, 2014.

887 Harden, J. W., Trumbore, S. E., Stocks, B. J., Hirsch, A., Gower, S. T., O'Neill, K. P., and
888 Kasischke, E. S.: The role of fire in the boreal carbon budget, *Glob. Change Biol.*, 6
889 (Supplement1), 174–184, doi:10.1046/j.1365-2486.2000.06019.x, 2000.

890 Hecobian, A., Liu, Z., Hennigan, C. J., Huey, L. G., Jimenez, J. L., Cubison, M. J., Vay, S.,
891 Diskin, G. S., Sachse, G. W., Wisthaler, A., Mikoviny, T., Weinheimer, A. J., Liao, J., Knapp, D.
892 J., Wennberg, P. O., Kürten, A., Crouse, J. D., Clair, J. St., Wang, Y., and Weber, R. J.:
893 Comparison of chemical characteristics of 495 biomass burning plumes intercepted by the
894 NASA DC-8 aircraft during the ARCTAS/CARB-2008 field campaign, *Atmos. Chem. Phys.*, 11,
895 13325–13337, doi:10.5194/acp-11-13325-2011, 2011.

896 Hegarty, J., Mao, H., and Talbot, R.: Synoptic controls on summertime surface ozone in the
897 northeastern United States, *J. Geophys. Res.-Atmos.*, 112, D14306, doi:10.1029/2006JD008170,
898 2007.

899 Hegarty, J., Mao, H., and Talbot, R.: Synoptic influences on springtime tropospheric O₃ and CO
900 over the North American export region observed by TES, *Atmos. Chem. Phys.*, 9, 3755–3776,
901 doi:10.5194/acp-9-3755-2009, 2009.

902 Herron-Thorpe, F. L., Mount, G. H., Emmons, L. K., Lamb, B. K., Jaffe, D. A., Wigder, N.
903 L., Chung, S. H., Zhang, R., Woelfle, M. D., and Vaughan, J. K.: Air quality simulations of
904 wildfires in the Pacific Northwest evaluated with surface and satellite observations during the
905 summers of 2007 and 2008, *Atmos. Chem. Phys.*, 14, 12533–12551, doi:10.5194/acp-14-12533-
906 2014, 2014.

907 Hess, P. G. and Lamarque, J. F.: Ozone source attribution and its modulation by the Arctic
908 oscillation during the spring months, *J. Geophys. Res.-Atmos.*, 112, 1–
909 17, doi:10.1029/2006JD007557, 2007.

910 Honrath, R. E., Owen, R. C., Val Martín, M., Reid, J. S., Lapina, K., Fialho, P., Dziobak, M. P.,
911 Kleissl, J., and Westphal, D. L.: Regional and hemispheric impacts of anthropogenic and
912 biomass burning emissions on summertime CO and O₃ in the North Atlantic lower free
913 troposphere, *J. Geophys. Res.-Atmos.*, 109, 1–17, doi:10.1029/2004JD005147, 2004.

914 Task Force on Hemispheric Transport of Air Pollution (TF HTAP): Hemispheric transport of air
915 pollution 2010 assessment report, edited by: Keating, T. J. and Zuber, A., draft, available at:
916 <http://www.htap.org>, 2010.

917 Hu, Q., Tawaye, Y., and Feng, S.: Variations of the Northern Hemisphere atmospheric energetics:
918 1948–2000, *J. Climate*, 17, 1975–1986, doi:10.1175/1520-
919 0442(2004)017<1975:VOTNHA>2.0.CO;2, 2004.

920 Hurrell, J. W.: Decadal trends in the north atlantic oscillation: regional temperatures and
921 precipitation, *Science*, 269, 676–679, doi:10.1126/science.269.5224.676, 1995.

922 Intergovernmental Panel on Climate Change (IPCC): *Climate Change 2001: The Scientific Basis*,
923 *Clim. Change 2001 Sci. Basis*, 881, doi:10.1256/004316502320517344, 2001.

924 Intergovernmental Panel on Climate Change (IPCC), *Climate Change 2007: The Physical*
925 *Science Basis*, in: *Contribution of Working Group I to the Fourth Assessment Report of the*
926 *Intergovernmental Panel on Climate Change*, edited by: Solomon, S., Qin, D., Manning, M.,
927 Chen, Z., Marquis, M., Averyt, K. B., Tignor M., and Miller H. L., Cambridge University Press,
928 Cambridge, UK and New York, NY, USA, 2007.

929 Jacob, D. J.: Seasonal transition from NO_x- to hydrocarbon-limited conditions for ozone
930 production over the eastern United States in september, *J. Geophys. Res.*, 100, 9315–9324,
931 doi:10.1029/94JD03125, 1995.

932 Jaffe, D., Bertsch, I., Jaeglé, L., Novelli, P., Reid, J. S., Tanimoto, H., Vingarzan, R., and
933 Westphal, D. L.: Long-range transport of Siberian biomass burning emissions and impact on
934 surface ozone in western North America, *Geophys. Res. Lett.*, 31, 6–9,
935 doi:10.1029/2004GL020093, 2004.

936 James, P., Stohl, A., Forster, C., Eckhardt, S., Seibert, P., and Frank, A.: A 15-year climatology
937 of stratosphere–troposphere exchange with a Lagrangian particle dispersion model 2. Mean
938 climate and seasonal variability, *J. Geophys. Res.-Atmos.*, 108,
939 8522, doi:10.1029/2002JD002639, 2003.

940 Jonson, J. E., Simpson, D., Fagerli, H., and Solberg, S.: Can we explain the trends in European
941 ozone levels?, *Atmos. Chem. Phys.*, 6, 51–66, doi:10.5194/acp-6-51-2006, 2006.

942 Kang, C. M., Gold, D., and Koutrakis, P.: Downwind O₃ and PM_{2.5} speciation during the
943 wildfires in 2002 and 2010, *Atmos. Environ.*, 95, 511–519,
944 doi:10.1016/j.atmosenv.2014.07.008,2014.

945 Kim, S.-W., Heckel, A., McKeen, S. A., Frost, G. J., Hsie, E.-Y., Trainer, M. K., Richter,
946 A.,Burrows, J. P., Peckham, S. E., and Grell, G. A.: Emission reductions and their impact on air
947 quality, *Geophys. Res. Lett.*, 33, 1–5, doi:10.1029/2006GL027749, 2006.

948 Kondragunta, S., Lee, P., McQueen, J., Kittaka, C., Prados, A. I., Ciren, P., Laszlo, I.,Pierce, R.
949 B., Hoff, R., and Szykman, J. J.: Air quality forecast verification using satellitedata, *J. Appl.*
950 *Meteorol. Clim.*, 47, 425–442, doi:10.1175/2007JAMC1392.1, 2008.

951 Kopacz, M., Jacob, D. J., Fisher, J. A., Logan, J. A., Zhang, L., Megretskaia, I. A., Yantosca, R.
952 M., Singh, K., Henze, D. K., Burrows, J. P., Buchwitz, M., Khlystova, I., McMillan, W. W.,
953 Gille, J. C., Edwards, D. P., Eldering, A., Thouret, V., and Nedelec, P.: Global estimates of CO
954 sources with high resolution by adjoint inversion of multiple satellite datasets(MOPITT, AIRS,
955 SCIAMACHY, TES), *Atmos. Chem. Phys.*, 10, 855–876, doi:10.5194/acp-10-855-2010, 2010.

956 Krichak, S. O. and Alpert, P.: Signatures of the NAO in the atmospheric circulation during wet
957 winter months over the Mediterranean region, *Theor. Appl. Climatol.*, 82, 27–
958 39,doi:10.1007/s00704-004-0119-7, 2005.

959 Kumar, A., Wu, S., Weise, M. F., Honrath, R., Owen, R. C., Helmig, D., Kramer, L., Val Martin,
960 M., and Li, Q.: Free-troposphere ozone and carbon monoxide over the North Atlantic for 2001–
961 2011, *Atmos. Chem. Phys.*, 13, 12537–12547, doi:10.5194/acp-13-12537-2013,2013.

962 Lai, T. L., Talbot, R., and Mao, H.: An investigation of two highest ozone episodes during the
963 last decade in New England, *Atmosphere*, 3, 59–86, doi:10.3390/atmos3010059, 2012.

964 Lamarque, J.-F., and Hess, P. G.: Arctic Oscillation modulation of the Northern Hemisphere
965 spring tropospheric ozone, *Geophys. Res. Lett.*, 31, L06127, doi:10.1029/2003GL019116,2004.

966 Lefohn, A. S., Shadwick, D., and Oltmans, S. J.: Characterizing changes in surface ozone levels
967 in metropolitan and rural areas in the United States for 1980–2008 and 1994–2008, *Atmos.*
968 *Environ.*, 44, 5199–5210, doi:10.1016/j.atmosenv.2010.08.049, 2010.

969 Leibensperger, E. M., Mickley, L. J., and Jacob, D. J.: Sensitivity of US air quality to mid-
970 latitude cyclone frequency and implications of 1980–2006 climate change, *Atmos. Chem. Phys.*,
971 8, 7075–7086, doi:10.5194/acp-8-7075-2008, 2008.

972 Liang, Q., Jaeglé, L., Jaffe, D. A., Weiss-Penzias, P., Heckman, A., and Snow, J. A.: Long-range
973 transport of Asian pollution to the northeast Pacific: seasonal variations and transport pathways
974 of carbon monoxide, *J. Geophys. Res.-Atmos.*, 109, 1–16, doi:10.1029/2003JD004402, 2004.

975 Li, Q., Jacob, D. J., Bey, I., Palmer, P. I., Duncan, B. N., Field, B. D., Martin, R. V., Fiore, A. M.,
976 Yantosca, R. M., Parrish, D. D., Simmonds, P. G. and Oltmans, S. J.: Transatlantic transport of
977 pollution and its effects on surface ozone in Europe and North America, *J. Geophys. Res.-*
978 *Atmos.*, 107, ACH 4-1–ACH 4-21, doi:10.1029/2001JD001422, 2002.

979 Li, Q., Jacob, D. J., Park, R., Wang, Y., Heald, C. L., Hudman, R., Yantosca, R. M., Martin, R.
980 V., and Evans, M.: North American pollution outflow and the trapping of convectively lifted
981 pollution by upper-level anticyclone, *J. Geophys. Res.-Atmos.*, 110, D10301,
982 doi:10.1029/2004JD005039, 2005.

983 Lin, C.-Y. C., Jacob, D. J., Munger, J. W., and Fiore, A. M.: Increasing background ozone in
984 surface air over the United States, *Geophys. Res. Lett.*, 27, 3465–3468,
985 doi:10.1029/2000GL011762, 2000.

986 Liu, J., Tarasick, D. W., Fioletov, V. E., McLinden, C., Zhao, T., Gong, S., Sioris, C., Jin, J. J.,
987 Liu, G., and Moeini, O.: A global ozone climatology from ozone soundings via trajectory
988 mapping: a stratospheric perspective, *Atmos. Chem. Phys.*, 13, 11441–11464, doi:10.5194/acp-
989 13-11441-2013, 2013.

990 Liu, S. C.: Ozone production in the rural troposphere and the implications for regional and global
991 ozone distributions., *J. Geophys. Res.*, 92, 4191–4207, 1987.

992 Logan, J. A.: Ozone in rural areas of the United States, *J. Geophys. Res.*, 94, 8511–8532, 1989.

993 Logan, J. A., Staehelin, J., Megretskaia, I. A., Cammas, J. P., Thouret, V., Claude, H., DeBacker,
994 H., Steinbacher, M., Scheel, H. E., Stbi, R., Fröhlich, M., and Derwent, R.: Changes in ozone
995 over Europe: analysis of ozone measurements from sondes, regular aircraft (MOZAIC) and alpine
996 surface sites, *J. Geophys. Res.-Atmos.*, 117, 1–23, doi:10.1029/2011JD016952, 2012.

997 Mao, H. and Talbot, R.: Role of meteorological processes in two New England ozone
998 episodes during summer 2001, *J. Geophys. Res.-Atmos.*, 109, 1–17,
999 doi:10.1029/2004JD004850, 2004.

1000 Mao, H. and Talbot, R.: Speciated mercury at marine, coastal, and inland sites in New England –
1001 Part 1: Temporal variability, *Atmos. Chem. Phys.*, 12, 5099–5112, doi:10.5194/acp-12-5099-
1002 2012, 2012.

1003 Mathur, R.: Estimating the impact of the 2004 Alaskan forest fires on episodic particular matter
1004 pollution over the eastern United States through assimilation of satellite-derived aerosol optical

1005 depths in a regional air quality model, *J. Geophys. Res.-Atmos.*, 113, D17302,
1006 doi:10.1029/2007JD009767, 2008.

1007 McKendry, I., Strawbridge, K., Karumudi, M. L., O'Neill, N., Macdonald, A. M., Leaitch,
1008 R., Jaffe, D., Cottle, P., Sharma, S., Sheridan, P., and Ogren, J.: Californian forest fire plumes
1009 over Southwestern British Columbia: lidar, sunphotometry, and mountaintop chemistry
1010 observations, *Atmos. Chem. Phys.*, 11, 465–477, doi:10.5194/acp-11-465-2011, 2011.

1011 Miller, S. M., Matross, D. M., Andrews, A. E., Millet, D. B., Longo, M., Gottlieb, E. W., Hirsch,
1012 A. I., Gerbig, C., Lin, J. C., Daube, B. C., Hudman, R. C., Dias, P. L. S., Chow, V. Y., and
1013 Wofsy, S. C.: Sources of carbon monoxide and formaldehyde in North America determined from
1014 high-resolution atmospheric data, *Atmos. Chem. Phys.*, 8, 7673–7696, doi:10.5194/acp-8-7673-
1015 2008, 2008.

1016 Monks, P.: A review of the observations and origins of the spring ozone maximum, *Atmos.*
1017 *Environ.*, 34, 3545–3561, doi:10.1016/S1352-2310(00)00129-1, 2000.

1018 Murazaki, K. and Hess, P.: How does climate change contribute to surface ozone change over
1019 the United States?, *J. Geophys. Res.-Atmos.*, 111, 1–16, doi:10.1029/2005JD005873, 2006.

1020 Novelli, P. C., Masarie, K. A., Lang, P. M., Hall, B. D., Myers, R. C., and Elkins, J. W.:
1021 Reanalysis of tropospheric CO trends: effects of the 1997–1998 wildfires, *J. Geophys. Res.-*
1022 *Atmos.*, 108, ACH 14-1–ACH 14-14, 2003.

1023 Oltmans, S. J., Lefohn, A. S., Harris, J. M., and Shadwick, D. S.: Background ozone levels of air
1024 entering the west coast of the US and assessment of longer-term changes, *Atmos. Environ.*, 42,
1025 6020–6038, doi:10.1016/j.atmosenv.2008.03.034, 2008.

1026 Oltmans, S. J., Lefohn, A. S., Harris, J. M., Tarasick, D. W., Thompson, A. M., Wernli, H.,
1027 Johnson, B. J., Novelli, P. C., Montzka, S. A., Ray, J. D., Patrick, L. C., Sweeney, C., Jefferson,

1028 A., Dann, T., Davies, J., Shapiro, M., and Holben, B. N.: Enhanced ozone over western North
1029 America from biomass burning in Eurasia during April 2008 as seen in surface and profile
1030 observations, *Atmos. Environ.*, 44, 4497–4509, doi:10.1016/j.atmosenv.2010.07.004, 2010.

1031 Oltmans, S. J., Lefohn, A. S., Shadwick, D., Harris, J. M., Scheel, H. E., Galbally, I., Tarasick, D.
1032 W., Johnson, B. J., Brunke, E. G., Claude, H., Zeng, G., Nichol, S., Schmidlin, F., Davies, J.,
1033 Cuevas, E., Redondas, A., Naoe, H., Nakano, T., and Kawasato, T.: Recent tropospheric ozone
1034 changes – a pattern dominated by slow or no growth, *Atmos. Environ.*, 67, 331–351,
1035 doi:10.1016/j.atmosenv.2012.10.057, 2013.

1036 Oswald, E. M., Dupigny-Giroux, L.-A., Leibensperger, E. M., Poirot, R., and Merrell, J.: Climate
1037 controls on air quality in the northeastern U.S.: an examination of summertime ozone statistics
1038 during 1993–2012, *Atmos. Environ.*, 112, 278–288, doi:10.1016/j.atmosenv.2015.04.019, 2015.

1039 Parrish, D. D., Singh, H. B., Molina, L., and Madronich, S.: Air quality progress in North
1040 American megacities: a review, *Atmos. Environ.*, 45, 7015–7025,
1041 doi:10.1016/j.atmosenv.2011.09.039, 2011.

1042 Parrish, D. D., Law, K. S., Staehelin, J., Derwent, R., Cooper, O. R., Tanimoto, H., Volz-Thomas,
1043 A., Gilge, S., Scheel, H.-E., Steinbacher, M., and Chan, E.: Long-term changes in lower
1044 tropospheric baseline ozone concentrations at northern mid-latitudes, *Atmos. Chem. Phys.*, 12,
1045 11485–11504, doi:10.5194/acp-12-11485-2012, 2012.

1046 Parrish, D. D., Law, K. S., Staehelin, J., Derwent, R., Cooper, O. R., Tanimoto, H., Volz-
1047 Thomas, A., Gilge, S., Scheel, H. E., Steinbacher, M., and Chan, E.: Lower tropospheric ozone at
1048 northern midlatitudes: changing seasonal cycle, *Geophys. Res. Lett.*, 40, 1631–1636,
1049 doi:10.1002/grl.50303, 2013.

1050 Pausata, F. S. R., Pozzoli, L., Vignati, E., and Dentener, F. J.: North Atlantic Oscillation and
1051 tropospheric ozone variability in Europe: model analysis and measurements intercomparison,
1052 *Atmos. Chem. Phys.*, 12, 6357–6376, doi:10.5194/acp-12-6357-2012, 2012.

1053 Penkett, S. A., Blake, N. J., Lightman, P., Marsh, A. R. W., Anwyl, P., and Butcher, G.: The
1054 seasonal variation of nonmethane hydrocarbons in the free troposphere over the North
1055 Atlantic Ocean: possible evidence for extensive reaction of hydrocarbons with the nitrate radical,
1056 *J. Geophys. Res.*, 98, 2865–2885, 1993.

1057 Petrenko, V. V., Martinerie, P., Novelli, P., Etheridge, D. M., Levin, I., Wang, Z., Blunier, T.,
1058 Chappellaz, J., Kaiser, J., Lang, P., Steele, L. P., Hammer, S., Mak, J., Langenfelds, R. L.,
1059 Schwander, J., Severinghaus, J. P., Witrant, E., Petron, G., Battle, M. O., Forster, G., Sturges, W.
1060 T., Lamarque, J.-F., Steffen, K., and White, J. W. C.: A 60 yr record of atmospheric carbon
1061 monoxide reconstructed from Greenland firn air, *Atmos. Chem. Phys.*, 13, 7567–7585,
1062 doi:10.5194/acp-13-7567-2013, 2013.

1063 Pfister, G., Hess, P. G., Emmons, L. K., Lamarque, J.-F., Wiedinmyer, C., Edwards, D. P.,
1064 Pétron, G., Gille, J. C., and Sachse, G. W.: Quantifying CO emissions from the 2004 Alaskan
1065 wildfires using MOPITT CO data, *Geophys. Res. Lett.*, 32, 1–5,
1066 doi:10.1029/2005GL022995, 2005.

1067 Pollack, I. B., Ryerson, T. B., Trainer, M., Neuman, J. A., Roberts, J. M., and Parrish, D. D.:
1068 Trends in ozone, its precursors, and related secondary oxidation products in Los Angeles,
1069 California: a synthesis of measurements from 1960 to 2010, *J. Geophys. Res.-Atmos.*, 118,
1070 5893–5911, doi:10.1002/jgrd.50472, 2013.

1071 Price, H. U., Jaffe, D. A., Cooper, O. R., and Doskey, P. V.: Photochemistry, ozone production,
1072 and dilution during long-range transport episodes from Eurasia to the northwest United States, *J.*
1073 *Geophys. Res.-Atmos.*, 109, 1–10, doi:10.1029/2003JD004400, 2004.

1074 Prinn, R. G.: The Cleansing Capacity of the Atmosphere, *Annu. Rev. Environ. Resour.*, 28, 29–
1075 57, doi:10.1146/annurev.energy.28.011503.163425, 2003.

1076 Racherla, P. N. and Adams, P. J.: The response of surface ozone to climate change over the
1077 Eastern United States, *Atmos. Chem. Phys.*, 8, 871–885, doi:10.5194/acp-8-871-2008, 2008.

1078 Real, E., Law, K. S., Weinzierl, B., Fiebig, M., Petzold, A., Wild, O., Methven, J., Arnold, S. A.,
1079 Stohl, A., Huntrieser, H., Roiger, A. E., Schlager, H., Stewart, D., Avery, M. A., Sachse, G.
1080 W., Browell, E. V., Ferrare, R. A., and Blake, D.: Processes influencing ozone levels in Alaskan
1081 forest fire plumes during long-range transport over the North Atlantic, *J. Geophys. Res.-Atmos.*,
1082 112, 1–19, doi:10.1029/2006JD007576, 2007.

1083 Reidmiller, D. R., Jaffe, D. A., Chand, D., Strode, S., Swartzendruber, P., Wolfe, G. M., and
1084 Thornton, J. A.: Interannual variability of long-range transport as seen at the Mt. Bachelor
1085 observatory, *Atmos. Chem. Phys.*, 9, 557–572, doi:10.5194/acp-9-557-2009, 2009.

1086 Rogers, J. C.: North Atlantic storm track variability and its association to the North Atlantic
1087 oscillation and climate variability of northern Europe, *J. Climate*, 10, 1635–
1088 1647, doi:10.1175/1520-0442(1997)010<1635:NASTVA>2.0.CO;2, 1997.

1089 Schwab, J. J., Spicer, J. B., and Demerjian, K. L.: Ozone, trace gas, and particulate matter
1090 measurements at a rural site in southwestern New York state: 1995–2005, *J. Air Waste Manage.*,
1091 59, 293–309, doi:10.3155/1047-3289.59.3.293, 2009.

1092 Serreze, M. C., Barrett, A. P., Slater, A. G., Steele, M., Zhang, J., and Trenberth, K. E.: The
1093 large-scale energy budget of the Arctic, *J. Geophys. Res.-Atmos.*, 112, 1–17,
1094 doi:10.1029/2006JD008230, 2007.

1095 Stevenson, D. S., Dentener, F. J., Schultz, M. G., Ellingsen, K., van Noije, T. P. C., Wild,
1096 O., Zeng, G., Amann, M., Atherton, C. S., Bell, N., Bergmann, D. J., Bey, I., Butler, T., Cofala, J.,
1097 Collins, W. J., Derwent, R. G., Doherty, R. M., Drevet, J., Eskes, H. J., Fiore, A. M., Gauss, M.,
1098 Hauglustaine, D. A., Horowitz, L. W., Isaksen, I. S. A., Krol, M. C., Lamarque, J. F., Lawrence,
1099 M. G., Montanaro, V., Müller, J. F., Pitari, G., Prather, M. J., Pyle, J. A., Rast, S., Rodriguez, J.
1100 M., Sanderson, M. G., Savage, N. H., Shindell, D. T., Strahan, S. E., Sudo, K., and Szopa, S.:
1101 Multimodel ensemble simulations of present-day and near-future tropospheric ozone, *J. Geophys.*
1102 *Res.-Atmos.*, 111, D08301, doi:10.1029/2005JD006338, 2006.

1103 Stohl, A., Bonasoni, P., Cristofanelli, P., Collins, W., Feichter, J., Frank, A., Forster, C.,
1104 Gerasopoulos, E., Gäggeler, H., James, P., Kentarchos, T., Kromp-Kolb, H., Krüger, B., Land,
1105 C., Meloen, J., Papayannis, A., Priller, A., Seibert, P., Sprenger, M., Roelofs, G. J., Scheel, H.
1106 E., Schnabel, C., Siegmund, P., Tobler, L., Trickl, T., Wernli, H., Wirth, V., Zanis, P., and
1107 Zerefos, C.: Stratosphere–troposphere exchange: a review, and what we have learned from
1108 STACCATO, *J. Geophys. Res.-Atmos.*, 108, 8516, doi:10.1029/2002JD002490, 2003.

1109 Talbot, R., Mao, H., and Sive, B.: Diurnal characteristics of surface level O₃ and other important
1110 trace gases in New England, *J. Geophys. Res.-Atmos.*, 110, 1–16, doi:10.1029/2004JD005449,
1111 2005.

1112 Thompson, D. W. J. and Wallace, J. M.: The Arctic oscillation signature in the wintertime
1113 geopotential height and temperature fields, *Geophys. Res. Lett.*, 25, 1297,
1114 doi:10.1029/98GL00950, 1998.

1115 Thompson, D. W. J. and Wallace, J. M.: Annular mode in the extratropical circulation. Part I:
1116 Month-to-month variability, *J. Climate*, 13, 1000–1016, 2000.

1117 Tilmes, S., Lamarque, J.-F., Emmons, L. K., Conley, A., Schultz, M. G., Saunois, M., Thouret,
1118 V., Thompson, A. M., Oltmans, S. J., Johnson, B., and Tarasick, D.: Technical Note:
1119 Ozonesonde climatology between 1995 and 2011: description, evaluation and applications,
1120 *Atmos. Chem. Phys.*, 12, 7475–7497, doi:10.5194/acp-12-7475-2012, 2012.

1121 Tohjima, Y., Kubo, M., Minejima, C., Mukai, H., Tanimoto, H., Ganshin, A., Maksyutov, S.,
1122 Katsumata, K., Machida, T., and Kita, K.: Temporal changes in the emissions of CH₄ and CO
1123 from China estimated from CH₄ / CO₂ and CO / CO₂ correlations observed at Hateruma Island,
1124 *Atmos. Chem. Phys.*, 14, 1663–1677, doi:10.5194/acp-14-1663-2014, 2014.

1125 U.S. Environmental Protection Agency (EPA): Our Nation’s Air Status and Trends Through
1126 2010, available at: <http://www3.epa.gov/airtrends/2011/>, 2012.

1127 U.S. Environmental Protection Agency (EPA): National Ambient Air Quality Standards for
1128 Ozone; Proposed Rule, *Fed. Regist.*, 79, 75234, doi:10.2753/RSH1061-1983310140, 2014.

1129 West, J. J., Fiore, A. M., Horowitz, L. W., and Mauzerall, D. L.: Global health benefits of
1130 mitigating ozone pollution with methane emission controls, *P. Natl. Acad. Sci. USA*, 103, 3988–
1131 3993, doi:10.1073/pnas.0600201103, 2006.

1132 Wigder, N. L., Jaffe, D. A., and Saketa, F. A.: Ozone and particulate matter enhancements from
1133 regional wildfires observed at Mount Bachelor during 2004–2011, *Atmos. Environ.*, 75, 24–31,
1134 doi:10.1016/j.atmosenv.2013.04.026, 2013.

1135 Wild, O. and Akimoto, H.: Intercontinental transport of ozone and its precursors in a three-
1136 dimensional global CTM, *J. Geophys. Res.-Atmos.*, 106, 27729–27744,
1137 doi:10.1029/2000JD000123, 2001.

1138 Wilson, R. C., Fleming, Z. L., Monks, P. S., Clain, G., Henne, S., Konovalov, I. B., Szopa, S.,
1139 and Menut, L.: Have primary emission reduction measures reduced ozone across Europe? An
1140 analysis of European rural background ozone trends 1996–2005, *Atmos. Chem. Phys.*, 12, 437–
1141 454, doi:10.5194/acp-12-437-2012, 2012.

1142 Woollings, T. and Blackburn, M.: The north Atlantic jet stream under climate change and its
1143 relation to the NAO and EA patterns, *J. Climate*, 25, 886–902, doi:10.1175/JCLI-D-11-00087.1,
1144 2012.

1145 Worden, H. M., Deeter, M. N., Frankenberg, C., George, M., Nichitiu, F., Worden, J., Aben, I.,
1146 Bowman, K. W., Clerbaux, C., Coheur, P. F., de Laat, A. T. J., Detweiler, R., Drummond, J. R.,
1147 Edwards, D. P., Gille, J. C., Hurtmans, D., Luo, M., Martínez-Alonso, S., Massie, S., Pfister, G.,
1148 and Warner, J. X.: Decadal record of satellite carbon monoxide observations, *Atmos. Chem.*
1149 *Phys.*, 13, 837–850, doi:10.5194/acp-13-837-2013, 2013.

1150 World Meteorological Organization: WMO Greenhouse Gas Bulletin: The State of Greenhouse
1151 Gases in the Atmosphere Based on Global Observations through 2011, No 8, 4, 2012.

1152 Wotawa, G. and Trainer, M.: The influence of Canadian forest fires on pollutant concentrations
1153 in the United States, *Science*, 288, 324–328, doi:10.1126/science.288.5464.324, 2000.

1154 Wotawa, G., Novelli, P. C., Trainer, M., and Granier, C.: Inter-annual variability of summertime
1155 CO concentrations in the Northern Hemisphere explained by boreal forest fires in North America
1156 and Russia, *Geophys. Res. Lett.*, 28, 4575–4578, doi:10.1029/2001GL013686, 2001.

1157 Xing, J., Pleim, J., Mathur, R., Pouliot, G., Hogrefe, C., Gan, C.-M., and Wei, C.: Historical
1158 gaseous and primary aerosol emissions in the United States from 1990 to 2010, *Atmos. Chem.*
1159 *Phys.*, 13, 7531–7549, doi:10.5194/acp-13-7531-2013, 2013.

1160 Xing, J., Mathur, R., Pleim, J., Hogrefe, C., Gan, C.-M., Wong, D. C., Wei, C., Gilliam, R., and
1161 Pouliot, G.: Observations and modeling of air quality trends over 1990–2010 across the Northern
1162 Hemisphere: China, the United States and Europe, *Atmos. Chem. Phys.*, 15, 2723–2747,
1163 doi:10.5194/acp-15-2723-2015, 2015.

1164 Xu, X., Lin, W., Wang, T., Yan, P., Tang, J., Meng, Z., and Wang, Y.: Long-term trend of
1165 surface ozone at a regional background station in eastern China 1991–2006: enhanced variability,
1166 *Atmos. Chem. Phys.*, 8, 2595–2607, doi:10.5194/acp-8-2595-2008, 2008.

1167 Zhang, Q., Streets, D. G., Carmichael, G. R., He, K. B., Huo, H., Kannari, A., Klimont, Z., Park,
1168 I. S., Reddy, S., Fu, J. S., Chen, D., Duan, L., Lei, Y., Wang, L. T., and Yao, Z. L.: Asian
1169 emissions in 2006 for the NASA INTEX-B mission, *Atmos. Chem. Phys.*, 9, 5131–5153,
1170 doi:10.5194/acp-9-5131-2009, 2009.

1171 Zhou, X., Huang, G., Civerolo, K., Roychowdhury, U., and Demerjian, K. L.: Summertime
1172 observations of HONO, HCHO, and O₃ at the summit of Whiteface Mountain, New York, J.
1173 *Geophys. Res.-Atmos.*, 112, 1–13, doi:10.1029/2006JD007256, 2007.

Table 1. Ground stations with geographical coordinates and measurement periods.

Site	Latitude	Longitude	Elevation	Measurement Period (CO)	Measurement Period (O ₃)
Appledore Island (AI)	42.97°N	70.62°W	18 m	Jul, 2001- Jul, 2011	Jul, 2002- Mar, 2012
Thompson Farm (TF)	43.11°N	70.95°W	23m	Apr, 2001- Jul, 2011	Apr, 2001- Aug, 2010
Mt. Washington (MWO)	44.27°N	71.30°W	1917m	Apr, 2001- Apr, 2009	Apr, 2001- May, 2010
Castle Spring (CS)	43.75°N	71.35°W	396m	Apr, 2001- Jun, 2008	Apr, 2001- May, 2008
Pack Monadnock (PM)	42.86°N	71.88°W	698m	Jun, 2004- Jul, 2011	Jul, 2004- Oct, 2008
Whiteface Mountain (WFM)	44.40°N	73.90°W	1484 m	Jan, 1996- Dec, 2010	Jan, 1996- Dec, 2010
Pinnacle State Park (PSP)	42.09°N	77.21°W	504 m	Jan, 1997- Dec, 2010	Jan, 1997- Dec, 2010

Note: CO and O₃ at AI were measured seasonally from May to September before 2007/2008. Year-round measurements of CO and O₃ began in May, 2007 and February, 2008, respectively.

Table 2. Trends (ppbv yr⁻¹) of baseline CO and O₃ in spring, summer, fall, and winter. *p*-values are in the parentheses. Boldfaced numbers indicate *p*-value < 0.10.

Site	Period	Spring		Summer		Fall		Winter		Annual	
		CO	O ₃	CO	O ₃	CO	O ₃	CO	O ₃	CO	O ₃
AI	2002-2010			0.8(0.66)	-3.1(0.07)						
CS	2001-2008	3.4(0.06)	0.9(0.65)	2.4(0.19)	-2.9(0.14)	1.1(0.57)	1.5(0.45)	6.1(<0.01)	0.4(0.86)	2.8(<0.01)	0.8(0.39)
MWO	2001-2009	-13.2(0.51)	-0.7(0.71)	-4.5(0.01)	-4.7(0.01)	-4.4(0.01)	-0.9(0.64)	-1.7(0.36)	0.1(0.98)	2.3(<0.01)	0.7(0.42)
PM	2005-2010	-6.5(<0.01)	-1.9(0.39)	-5.5(<0.01)	-3.5(0.14)	-4.2(0.05)	-3.4(0.11)	-5.5(0.01)	0.1(1.00)	3.5(<0.01)	0.8(0.43)
TF	2001-2010	-3.7(0.02)	2.4(0.10)	-4.5(<0.01)	-0.1(0.94)	-3.2(0.04)	0.2(0.90)	-4.8(<0.01)	2.7(0.09)	2.5(<0.01)	0.8(0.29)
PSP	2001-2010	-4.5(<0.01)	1.3(0.43)	-4.3(<0.01)	-0.8(0.57)	-4.2(0.01)	-1.9(0.23)	-3.9(0.02)	-0.7(0.68)	4.3(<0.01)	0.7(0.40)
WFM	2001-2010	-0.5(0.78)	0.4(0.83)	-1.9(0.23)	-4.7(<0.01)	-6.4(<0.01)	0.5(0.76)	-2.1(0.21)	-1.3(0.45)	2.8(<0.01)	0.9(0.27)

Table 3. The contributions, in r^2R^2 , of CO emissions from wildfires over Russia, Canada, Alaska, and California to variation (r^2) in baseline CO at each site. The combined effect of wildfire emissions over Russia and Canada was also computed. Boldfaced numbers indicate p -value < 0.10.

	Russia		Canada		Alaska		California		Combined	
	r^2R^2	p	r^2R^2	p	r^2R^2	p	r^2R^2	p	r^2R^2	p
AI	0.39	0.01	0.12	0.15	0.13	0.19	0.12	0.21	0.41	0.02
CS	-0.41	-0.01	-0.17	-0.09	-0.06	-0.38	<0.01	-0.92	-0.41	-0.02
MWO	0.41	0.01	0.13	0.15	0.01	0.77	<0.01	0.88	0.43	0.02
TF	0.64	0.01	0.40	0.05	0.01	0.80	0.03	0.52	0.65	0.01
PSP	0.11	0.18	0.15	0.11	0.09	0.27	<0.01	0.93	0.16	0.27
WFM	0.32	0.01	0.32	0.01	<0.01	0.90	0.01	0.69	0.38	0.03
Mean	0.37	0.38	0.22		<0.05		<0.03		0.41	

Note: PM was not included due to insufficient data; CS was not included, as mixing ratios of baseline CO at this site were unusually high over May 2003 – June 2008.

Table 4. Correlation coefficient (r) and p-value between the pairs of variables in March and April over 2001 – 2010.

<u>Pair of Variables</u>	<u>CS</u>	<u>MWO</u>	<u>PM</u>	<u>TF</u>	<u>PSP</u>	<u>WFM</u>
<u>NAO index vs Baseline O₃</u>	<u>-0.75 (0.03)</u>	<u>-0.68 (0.03)</u>	<u>-0.81 (0.03)</u>	<u>-0.81 (<0.01)</u>	<u>-0.58 (0.06)</u>	<u>-0.51 (0.10)</u>
<u>NAO index vs Baseline CO</u>	=	<u>-0.51 (0.12)</u>	<u>-0.06 (0.46)</u>	<u>0.30 (0.22)</u>	<u>-0.14 (0.36)</u>	<u>-0.16 (0.34)</u>
<u>Relative humidity vs NAO index</u>	<u>0.85 (0.02)</u>	=	=	<u>0.64 (0.06)</u>	<u>0.23 (0.26)</u>	<u>0.40 (0.13)</u>
<u>Relative humidity vs Solar radiation flux</u>	=	=	=	<u>-0.67 (0.05)</u>	=	=
<u>Baseline O₃ vs Solar radiation flux</u>	=	=	=	<u>0.75 (0.03)</u>	=	=
<u>Surface wind speed vs NAO index</u>	<u>0.68 (0.06)</u>	<u>0.76 (0.02)</u>	=	<u>0.57 (0.09)</u>	<u>0.44 (0.12)</u>	=

Note: CO at CS was not included, as mixing ratios of baseline CO at this site were unusually high over May 2003 – June 2008.

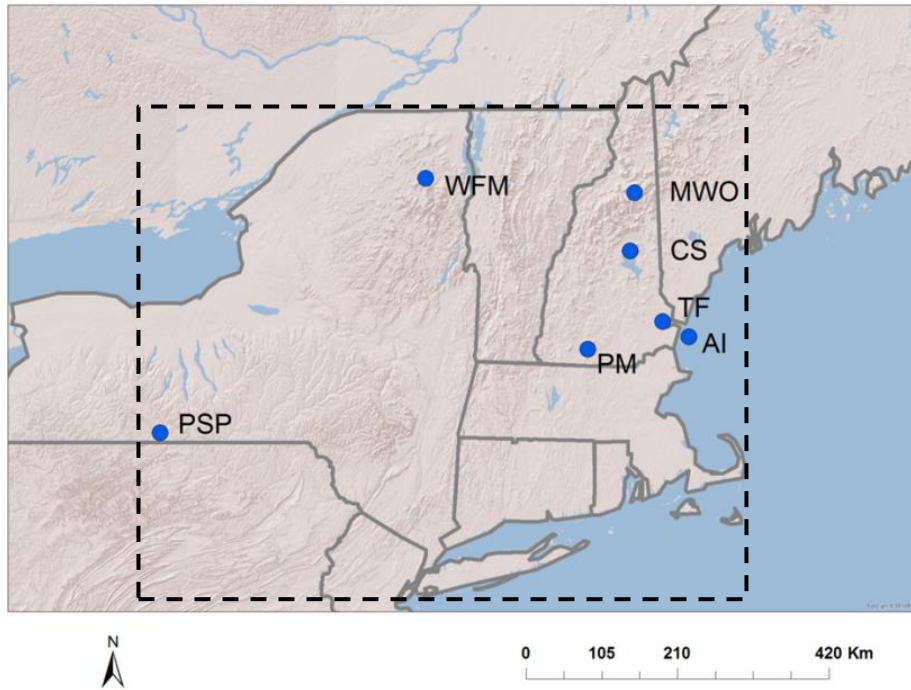


Fig. 1. Map of the Northeast U.S. The seven measurement sites used in the study are marked with blue dots.

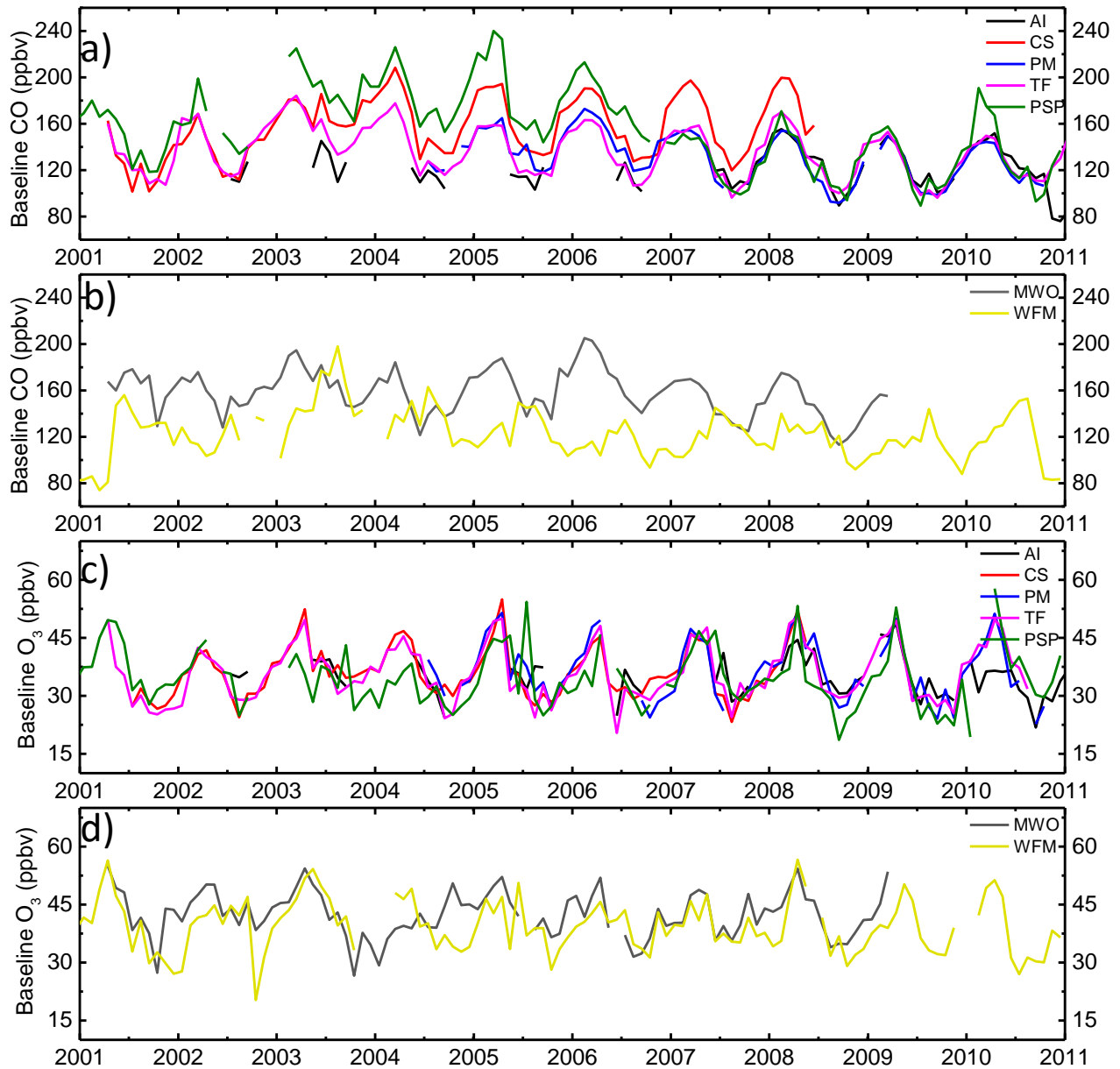


Fig. 2. Monthly baseline CO (ppbv) at (a) AI, CS, ~~MWO~~, PM, ~~and~~ TF, and PSP, and (b) MWO and WFM~~PSP~~. Monthly baseline O₃ (ppbv) at (c) AI, CS, ~~MWO~~, PM, ~~and~~ TF, and PSP, and (d) MWO and WFM~~PSP~~.

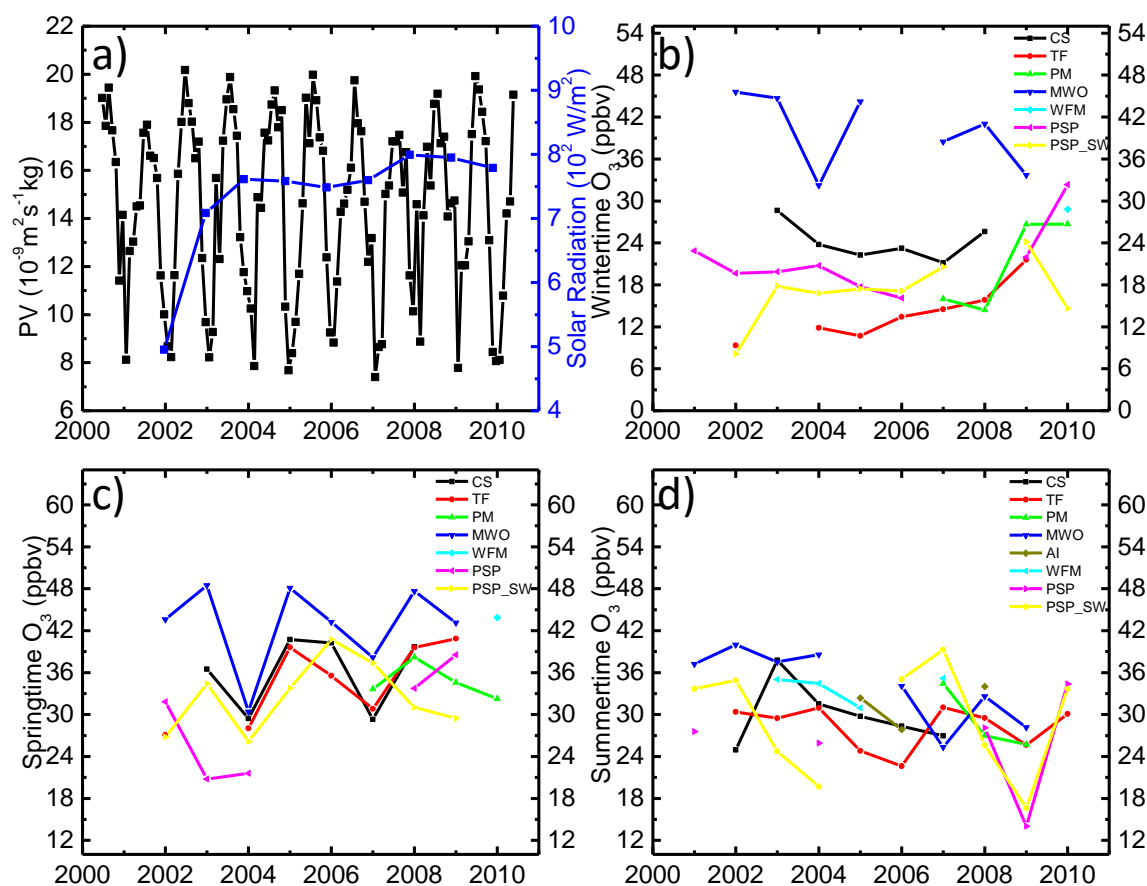


Fig. 3. (a) Time series of monthly PV ($10^{-9} \text{ m}^2 \text{ s}^{-1} \text{ kg}$) at 350 K over the study region ($40^\circ\text{N} - 45^\circ\text{N}$, $70^\circ\text{W} - 77.5^\circ\text{W}$), indicated with dashed box in Fig. 1) and averaged daily maximum solar radiation flux at TF in spring (March, April, and May). Seasonal 10th percentile mixing ratios of O_3 with wind from the directions aligned with the urban corridor in (b) winter, (c) spring, and (d) summer. Specifically, the wind directions selected for AI: $157.5^\circ - 202.5^\circ$; CS: $157.5^\circ - 202.5^\circ$; MWO: $157.5^\circ - 202.5^\circ$; PM: $112.5^\circ - 157.5^\circ$; TF: $157.5^\circ - 202.5^\circ$; WFM: $112.5^\circ - 157.5^\circ$; PSP: $67.5^\circ - 112.5^\circ$. In addition, seasonal 10th percentile mixing ratios of O_3 at PSP with wind from the directions aligned with the Ohio River Valley was calculate as PSP_SW ($202.5^\circ - 247.5^\circ$) in (b), (c), and (d).

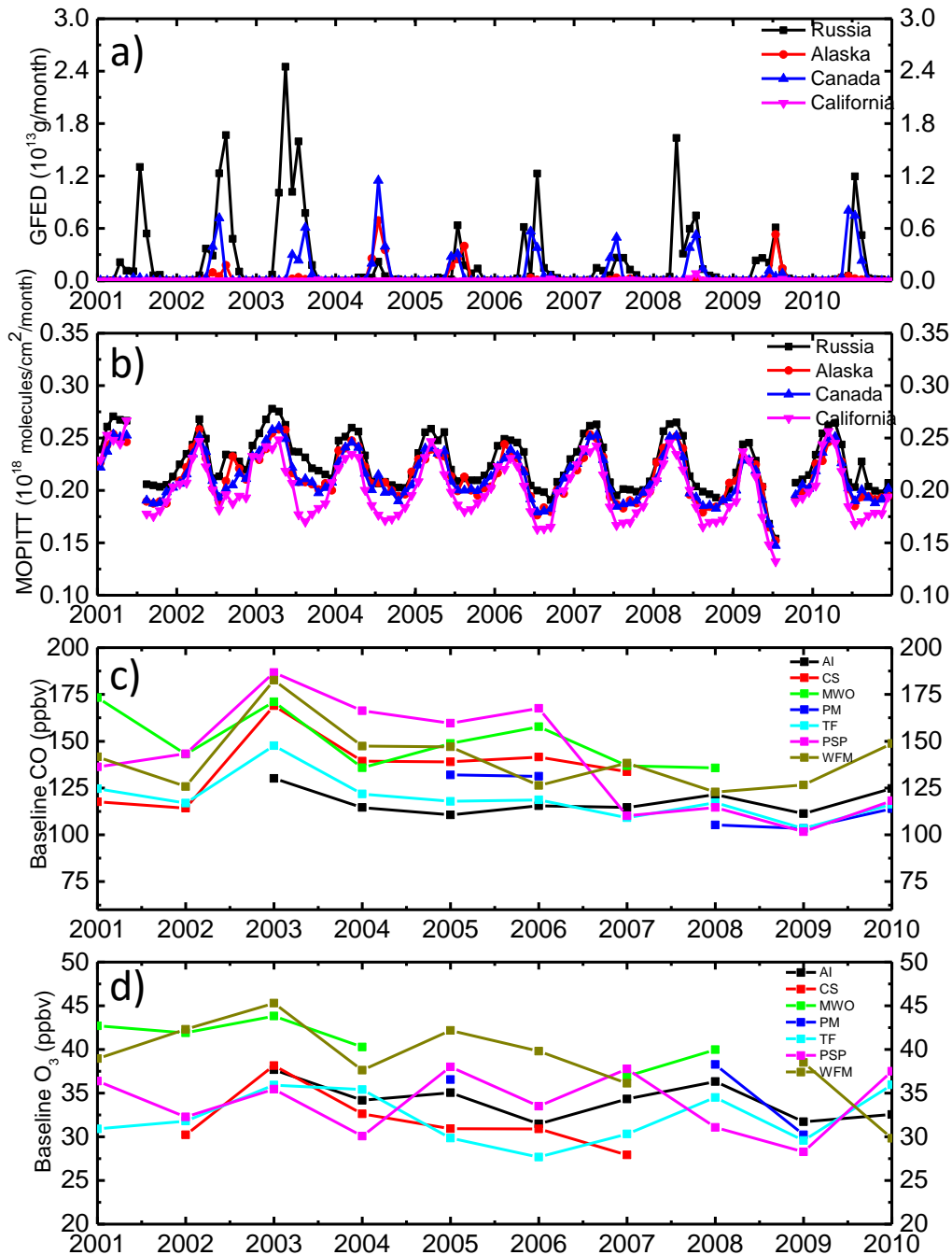


Fig. 4. (a) CO emissions from biomass burning based on GFED dataset. (b) Total CO columns based on MOPITT retrievals over Russia (black), Alaska (red), Canada (blue), and California (magenta). Summertime averaged baseline (c) CO and (d) O₃ at each site.

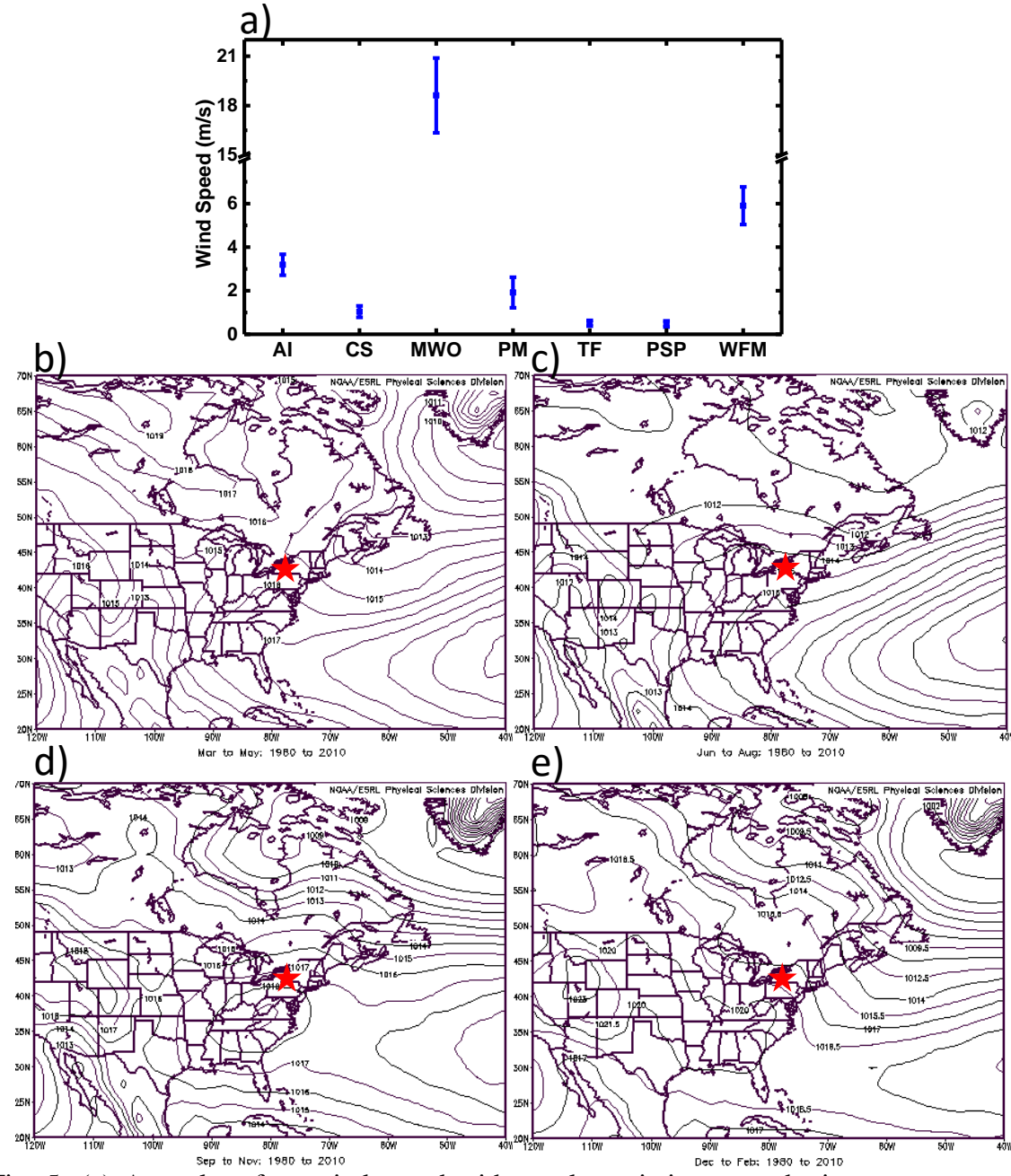


Fig. 5. (a) Annual surface wind speed with yearly variation at each site over summer 2001 – 2010. Northeast U.S. sea surface pressure (hPa) in (b) spring, (c) summer, (d) fall, and (e) winter. Red stars indicate the location of PSP.

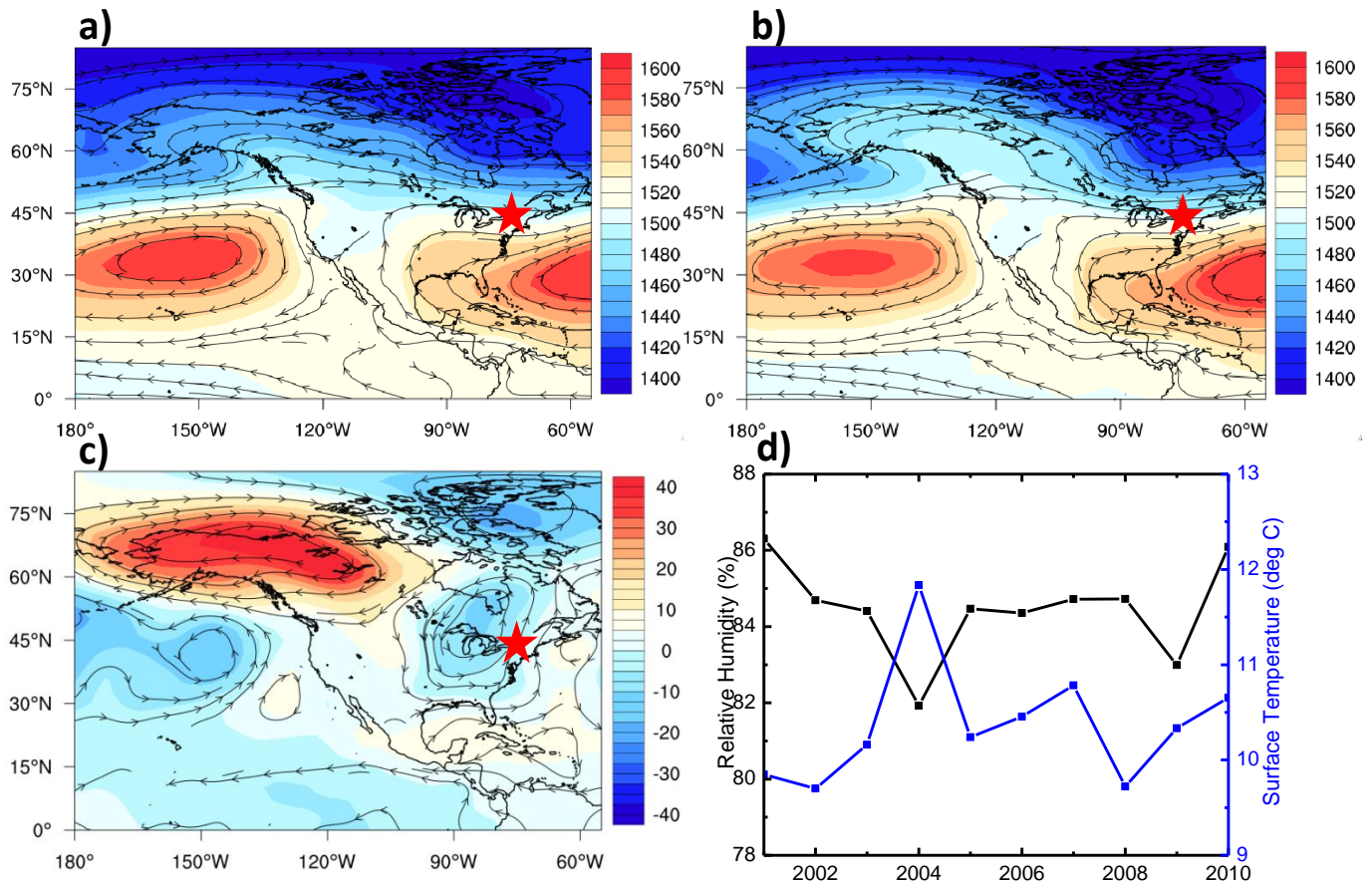


Fig. 6. Geopotential height at the 850 hPa pressure level during summer in (a) 2001-2010 (b) 2004. (c) The difference of geopotential height at 850 hPa between summer 2004 and the 10-year average. (d) The annual surface temperature and relative humidity over Alaska and southwestern Canada (55°N – 70°N, 110°W – 160°W) over summer 2001 – 2010. Red stars indicated the area of the study sites. (Source: NCEP/NCAR reanalysis)

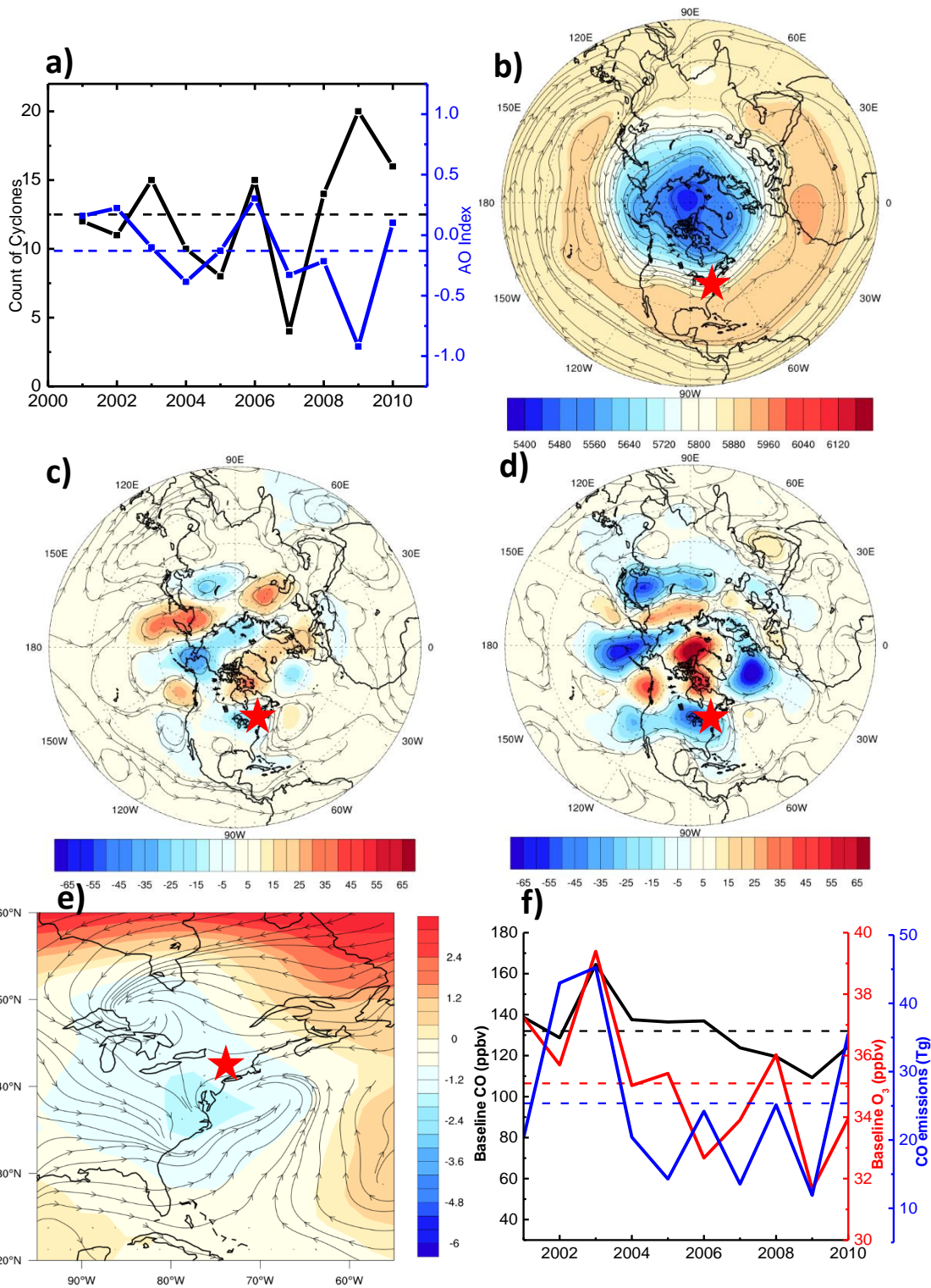


Fig. 7. (a) Counts of cyclones in the Northeast U.S. (black) and the AO index (blue) in summer. (b) Geopotential height at 500 hPa from the NCEP/NCAR reanalysis data during summer 2001 – 2010. (c) The difference of geopotential height at 500 hPa between years with strong (2003, 2006, 2008, 2009, and 2010) and weak (2001, 2002, 2004, 2005, and 2007) cyclone activities. (d) The difference of geopotential height at 500 hPa between summer 2009 and the 10-year means. (e) The difference of sea level pressure between summer 2009 and the 10-year means. (f) Time series of summertime baseline CO (black) and baseline O₃ (red) averaged over all seven sites, and Time series of CO emissions (blue) from wildfires in Russia and Canada. Dashlines indicate the 10-year means. Red stars indicate the area of the study sites.

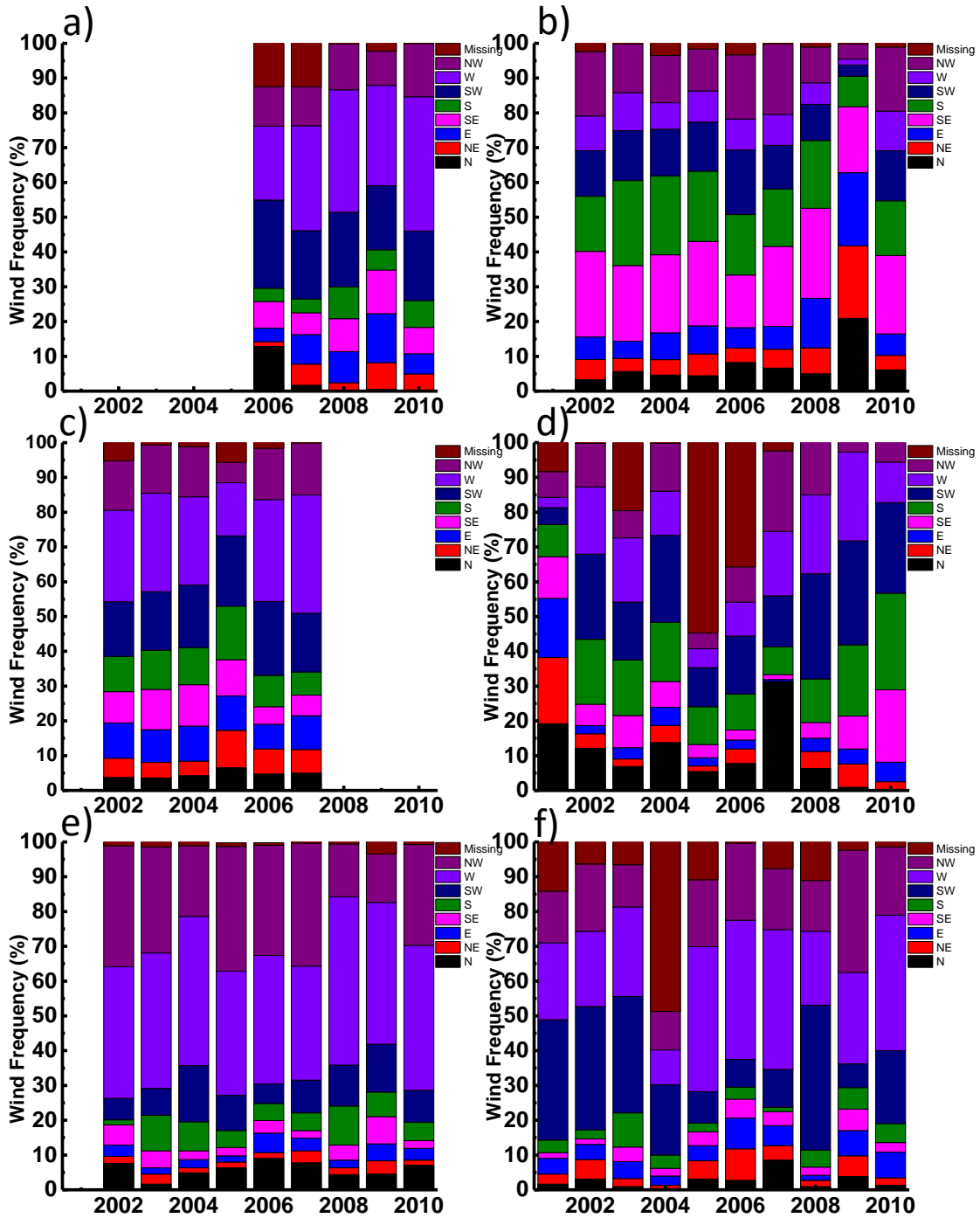


Fig. 8. Wind frequency in summer at (a) PM, (b) MWO, (c) CS, (d) WFM, (e) TF, (f) PSP. N:-
 22.5° – 22.5°; NE: 22.5° – 67.5°; E: 67.5° – 112.5°; SE: 112.5° – 157.5°; S: 157.5° – 202.5°; SW:
 202.5° – 247.5°; W: 247.5° – 337.5°; NW: 337.5° – -22.5°

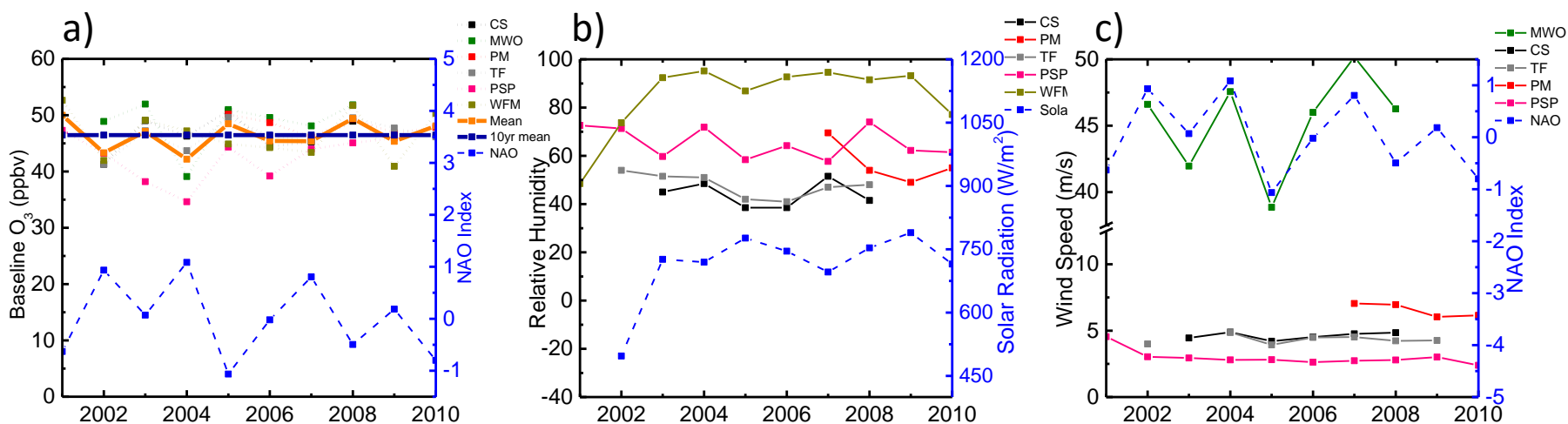


Fig. 9. (a) Baseline O₃ and the NAO index averaged in March and April. The thick orange line indicates the baseline O₃ averaged over the seven sites and the thick dark blue line indicates the mean value 46.5 ppbv over 2001 – 2010. (b) Averaged daytime (18:00 – 24:00 UT) relative humidity and daily maximum solar radiation flux at TF in March and April. (c) Averaged wind speed (> 2 m s⁻¹) from the west (247.5° – 337.5°) and the NAO index in March and April.

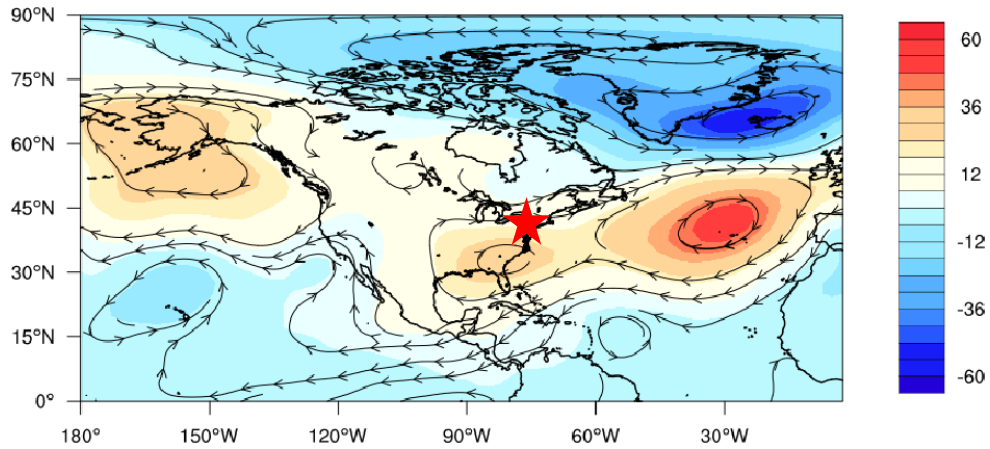


Fig. 10. The difference of geopotential height (m) and streamlines at 850-hPa between the low O_3 years (2002, 2004, 2006, 2007, and 2009) and high O_3 years (2001, 2003, 2005, 2008, and 2010). The red star indicates the area including the study sites.

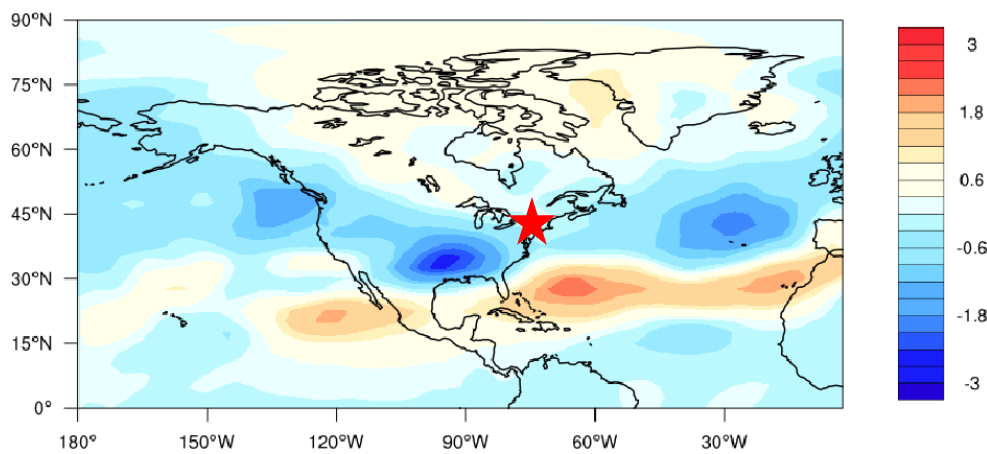


Fig. 11. Same as Fig. 10 except that the difference of PV ($10^{-9} \text{ m}^2 \text{ s}^{-1} \text{ kg}$) at 350 K is shown.

